Geochronology and tectonic context of lithium-cesium-tantalum pegmatites in the Appalachians

by

D. Bradley, E. Shea, R. Buchwaldt, S. Bowring, J. Benowitz, P. O'Sullivan, and A. McCauley

APPENDIX A

ANALYTICAL METHODS—U-Pb CA-TIMS Geochronology at Massachusetts Institute of Technology

Separation of heavy minerals from all samples followed standard crushing, heavy liquid, and magnetic separation techniques. Zircon crystals were picked in ethanol under a binocular microscope and were selected based on their morphology, color, clarity, and lack of inclusions. Zircons selected for U-Pb analysis were placed in quartz beakers and annealed in a muffle furnace at 900 ± 20 °C for 60 hours following this step, zircons were chemically abraded using a modified version of the technique of (Mattinson, 2005). Grains were loaded in 300 μl Teflon FEP microcapsules, placed in a Parr vessel, and leached in ~120 μl of 29 M HF for 12 hours at 220 °C. Following the leach step, grains were fluxed in HNO_3 for 30 minutes and then sonicated for 45 minutes. After this step, grains were rinsed two times in ultrapure water and fluxed in 6 M HCl for 30 minutes and sonicated for 45 minutes. Grains were each rinsed two more times in ultrapure water and then loaded into individual microcapsules with ~120 μl of 29 M HF and a mixed ^{205}Pb-^{233}U-^{235}U spike (ET535). Zircons were dissolved at 220 °C for 48 hours, dried to salts, and re-dissolved in ~120 μl of 6 M HCl at 180 °C for at least 12 hours. Pb and U were separated from the sample using HCl-based anion exchange columns modified from (Krogh, 1973).

Pb and U were analyzed by thermal ionization mass spectrometry on the MIT VG Sector 54 multicollector mass spectrometer or the MIT Isotopx X62 multicollector mass spectrometer. Both Pb and U were loaded onto degassed single zone-refined Re filaments with a silica gel-H_3PO_4 mixture (Gerstenberger and Haase, 1997). Pb was measured by peak-hopping on a single Daly detector. U was measured in static Faraday mode. Isotope ratios Pb were corrected for mass fractionation during analysis using the ET535 tracer solution (McLean et al., 2015; Condon et al., 2015). Data aquisiton and reduction was accomplished using the Tripoli and U-Pb Redux software packages (McLean et al., 2011; Bowring et al., 2011).

Calculated U-Pb dates are reported at 95% confidence level (Table 3 and Figure 7). Zircon dates are interpreted using the $^{206}Pb/^{238}U$ dates, which give the highest possible precision for rocks of this general age range. The $^{206}Pb/^{238}U$ dates are calculated with the decay constants of Jaffey et al. (1971) and the present day $^{238}U/^{235}U$ ratio recommended by Hiess et al. (2012); errors were calculated using the algorithms of McLean et al. (2011). All dates are corrected for initial ^{230}Th disequilibrium using an average whole rock Th/U ratio of 2.8. Uncertainties in U-Pb dates are reported as ±X/Y/Z, where X is the internal (analytical) uncertainty in the absence of all external errors, Y incorporates the U-Pb tracer calibration error and Z includes the latter as well as the decay constant errors of Jaffey and others (1971). The external uncertainties must be taken into account if the results are to be compared with U-Pb dates obtained in other laboratories with different tracers (Y) or ones derived from other isotopic chronometers (Z).

APPENDIX B

ANALYTICAL METHODS—$^{40}Ar/^{39}Ar$ geochronology at University of Alaska Fairbanks

For $^{40}Ar/^{39}Ar$ analysis, pegmatite samples were submitted to the Geochronology laboratory at UAF where they were crushed, sieved, washed and hand-picked for muscovite mineral phases. The monitor mineral MMhb-1 (Samson and Alexander, 1987) with an age of 513.9 Ma (Lanphere and Dalrymple, 2000) was used to monitor neutron flux (and calculate the irradiation parameter, J). The samples and standards were wrapped in aluminum foil and loaded into aluminum cans of 2.5 cm diameter and 6 cm height. The samples were irradiated in position 5c of the uranium enriched research reactor of McMaster University in Hamilton, Ontario, Canada for 20 megawatt-hours.

Upon their return from the reactor, the samples and monitors were loaded into 2 mm diameter holes in a copper tray that was then loaded in a ultra-high vacuum extraction line. The monitors were fused, and samples heated, using a 6-watt argon-ion laser following the technique described in York et al. (1981), Layer et al. (1987) and Layer (2000). Argon purification was achieved using a liquid nitrogen cold trap and a SAES Zr-Al getter at 400C. The samples were analyzed in a VG-3600 mass spectrometer at the Geophysical Institute, University of Alaska Fairbanks. The argon isotopes measured were corrected for system blank and mass discrimination, as well as calcium, potassium and chlorine interference reactions following procedures outlined in McDougall and Harrision (1999). System blanks generally were $2x10^{-16}$ mol ^{40}Ar and $2x10^{-18}$ mol ^{36}Ar which are 10 to 50 times smaller than fraction volumes. Mass discrimination was monitored by running both calibrated air shots and a zero-age glass sample. These measurements were made on a weekly to monthly basis to check for changes in mass discrimination.

A summary of all the $^{40}Ar/^{39}Ar$ results is given in the paper in Table 2, with all ages quoted to the +/- 1 sigma level and calculated using the constants of Steiger and Jaeger (1977). The integrated age is the age given by the total gas measured and is equivalent to a potassium-argon (K-Ar) age. The spectrum provides a plateau age if three or more consecutive gas fractions represent at least 50% of the total gas release and are within two standard deviations of each other (Mean Square Weighted Deviation less than 2.5).

Argon analytical data are presented in Table B1. Additional plots are shown in Figure B1.

Table B1. Argon analytical data.

10ADW500A MU#L1

Weighted average of J from standards = 3.954e-03 +/- 2.790e-05

Laser Power (mW)	Cumulative 39Ar	40Ar/39Ar measured	+/-	37Ar/39Ar measured	+/-	36Ar/39Ar measured	+/-	% Atmosphe 40Ar	Ca/K	+/-	Cl/K	+/-	40*/39K	+/-	Age (Ma)	+/- (Ma)
300	0.0024	33.74484	4.85556	-0.05388	0.07092	0.0493	0.05585	43.21923	-0.09885	0.13012	-0.00343	0.00614	19.14298	17.13781	131.64	113.65
500	0.0056	32.62678	3.47466	-0.04287	0.06824	-0.01184	0.04951	-10.72286	-0.07866	0.1252	-0.00648	0.00455	36.09133	15.04627	240.67	93.93
750	0.0198	42.92302	0.94291	-0.00326	0.0153	0.00076	0.01032	0.52431	-0.00598	0.02807	-0.00156	0.00106	42.66832	3.19095	281.27	19.48
1000	0.0274	42.36415	1.46504	-0.05864	0.02422	-0.0206	0.01317	-14.3709	-0.1076	0.04444	-0.0018	0.00217	48.41628	4.18021	316.02	25.03
1250	0.04	40.20492	0.94903	0.00083	0.01417	-0.00341	0.01087	-2.50854	0.00152	0.026	0.00008	0.00108	41.18306	3.35283	272.18	20.57
1500	0.2719	40.56851	0.82418	-0.00046	0.00106	0.00113	0.00053	0.82553	-0.00085	0.00194	0.0003	0.00009	40.20414	0.83577	266.17	5.14
2000	0.4415	39.78761	0.79336	0.00051	0.00107	0.00062	0.0008	0.45788	0.00094	0.00197	0.00015	0.00012	39.57588	0.8261	262.3	5.1
2500	0.5008	40.72375	0.70884	-0.00062	0.00386	0.00284	0.00218	2.06424	-0.00113	0.00708	-0.00024	0.00035	39.854	0.94903	264.01	5.85
3000	0.8021	41.89114	0.87861	0.00078	0.001	0.00154	0.00048	1.08647	0.00144	0.00183	0.00033	0.00007	41.40666	0.885	273.55	5.43
4000	0.9853	41.58118	0.87108	-0.00117	0.00123	0.00101	0.00058	0.71598	-0.00215	0.00226	0.00033	0.00013	41.25394	0.88385	272.62	5.42
9000	1	42.19686	0.85822	-0.00625	0.01315	-0.00322	0.00877	-2.25445	-0.01148	0.02412	-0.00058	0.00095	43.11761	2.73252	284.01	16.65
Integrated		41.05358	0.39004	-0.00088	0.00072	0.00103	0.00044	0.7402	-0.00162	0.00132	0.00017	0.00006	40.7202	0.40958	269.34	3.07

10ADW501B MU#L1

Weighted average of J from standards = 3.954e-03 +/- 2.790e-05

Laser Power (mW)	Cumulative 39Ar	40Ar/39Ar measured	+/-	37Ar/39Ar measured	+/-	36Ar/39Ar measured	+/-	% Atmosphe 40Ar	Ca/K	+/-	Cl/K	+/-	40*/39K	+/-	Age (Ma)	+/- (Ma)
500	0.0011	109.55354	4.36191	0.10856	0.03843	0.32029	0.02318	86.40705	0.19921	0.07052	-0.00371	0.00505	14.88867	6.17749	103.2	41.62
800	0.0049	43.6598	0.58579	0.00459	0.00928	0.03259	0.00774	22.07283	0.00842	0.01703	-0.00021	0.00118	33.99982	2.34305	227.57	14.73
1200	0.8779	35.43918	0.46347	0.00008	0.00008	0.00236	0.00005	1.96789	0.00015	0.00015	0.00047	0.00005	34.71267	0.4553	232.05	2.86
1500	0.9597	35.01106	0.71872	0.00041	0.00057	0.00307	0.00029	2.59723	0.00076	0.00105	0.00036	0.0001	34.07282	0.71444	228.03	4.49
2000	0.9786	35.21393	0.61363	-0.00341	0.0023	0.00184	0.00125	1.54493	-0.00625	0.00423	0.00034	0.0003	34.64058	0.71018	231.59	4.46
2500	0.9892	34.9456	0.56701	-0.00268	0.00508	0.00102	0.00246	0.86264	-0.00492	0.00933	0.00023	0.00035	34.61463	0.9203	231.43	5.77
3000	0.9959	34.71329	0.60133	-0.00163	0.00532	-0.00398	0.00381	-3.39229	-0.00298	0.00975	0.00033	0.00062	35.86012	1.28426	239.23	8.02
5000	0.9984	35.35911	0.74474	-0.0145	0.01506	-0.00346	0.00892	-2.89173	-0.0266	0.02763	-0.00249	0.00159	36.35067	2.74075	242.29	17.09
9000	1	35.8512	1.32131	-0.00919	0.02165	-0.00011	0.01127	-0.09165	-0.01685	0.03972	-0.00289	0.00282	35.8541	3.58176	239.19	22.38
Integrated		35.50091	0.4098	0.00008	0.00014	0.00279	0.00008	2.32152	0.00015	0.00025	0.00044	0.00004	34.64774	0.40183	231.64	2.95

11DW1 MU#L1

Weighted average of J from standards = 3.954e-03 +/- 2.790e-05

Laser Power (mW)	Cumulative 39Ar	40Ar/39Ar measured	+/-	37Ar/39Ar measured	+/-	36Ar/39Ar measured	+/-	% Atmosphe 40Ar	Ca/K	+/-	Cl/K	+/-	40*/39K	+/-	Age (Ma)	+/- (Ma)
500	0.0009	63.8961	3.04674	0.22113	0.04007	0.12987	0.02075	60.05878	0.40581	0.07354	0.00477	0.00303	25.513	6.31264	173.4	40.91
800	0.0041	42.58627	0.67847	0.06454	0.01257	0.013	0.0071	9.01551	0.11842	0.02307	0.00013	0.00126	38.72164	2.19336	257.02	13.57
1200	0.0164	50.87786	0.92737	0.02569	0.00317	0.00914	0.0016	5.3068	0.04713	0.00582	0.0002	0.00023	48.15062	1.0158	314.43	6.09
1500	0.2029	58.17971	0.86824	0.00199	0.00021	0.00739	0.00015	3.75426	0.00365	0.00039	0.00034	0.00005	55.96699	0.84128	360.67	4.91

2000	0.6883	55.52415	0.73066	0.00592	0.00015	0.00052	0.00006	0.27438	0.01087	0.00028	0.00026	0.00003	55.34241	0.72927	357.02	4.27
2500	0.8913	56.35649	0.79627	0.06443	0.00109	0.00061	0.00014	0.31021	0.11823	0.00199	0.00041	0.00005	56.15462	0.79531	361.77	4.64
3000	0.9222	54.18901	0.99497	0.02546	0.00143	0.00098	0.00064	0.5323	0.04671	0.00263	0.0003	0.0001	53.87199	1.01029	348.39	5.94
5000	0.9847	52.95443	0.81658	0.05544	0.00121	0.00104	0.00035	0.57024	0.10172	0.00222	0.00028	0.00006	52.625	0.81932	341.04	4.84
9000	1	55.66744	0.96173	0.08901	0.00294	0.00005	0.00112	0.01301	0.16333	0.00539	0.00068	0.00021	55.63401	1.01747	358.73	5.95
Integrated		55.89806	0.42617	0.02267	0.00025	0.00212	0.00007	1.11934	0.04159	0.00046	0.00032	0.00002	55.24389	0.42277	356.44	3.37

11DW5A MU#L1

Weighted average of J from standards = 3.954e-03 +/- 2.790e-05

Laser Power (mW)	Cumulative 39Ar	40Ar/39Ar measured	+/-	37Ar/39Ar measured	+/-	36Ar/39Ar measured	+/-	% Atmosphe 40Ar	Ca/K	+/-	Cl/K	+/-	40*/39K	+/-	Age (Ma)	+/- (Ma)
1500	0.0037	132.12955	2.09139	-0.00835	0.01571	0.11816	0.00845	26.43243	-0.01531	0.02883	0.00317	0.00129	97.18207	2.9531	586.65	15.22
3000	0.5508	74.44729	1.00077	0.0004	0.00018	0.02331	0.00034	9.25427	0.00074	0.00033	0.00028	0.00005	67.53081	0.91769	426.98	5.17
3250	0.6088	63.52463	1.23653	0.00054	0.00123	0.00822	0.00077	3.82701	0.00099	0.00226	0.00033	0.00012	61.06499	1.23239	390.21	7.08
3500	0.6631	61.52755	1.15745	0.00012	0.00126	0.00075	0.00057	0.36154	0.00023	0.00232	0.00034	0.00011	61.27551	1.16766	391.42	6.71
3750	0.7204	61.08334	1.18033	-0.0015	0.00138	0.00081	0.00061	0.39216	-0.00274	0.00254	0.00029	0.00011	60.81414	1.19192	388.76	6.85
4000	0.7756	60.27601	1.18935	0.00047	0.00109	0.00243	0.00096	1.19222	0.00086	0.002	0.00019	0.0001	59.52806	1.21574	381.35	7.02
4250	0.8096	58.15431	1.08336	-0.00163	0.00181	-0.00156	0.00078	-0.79231	-0.00299	0.00333	0.00022	0.00014	58.58506	1.11267	375.9	6.44
4500	0.8389	56.40483	0.94675	-0.00344	0.0027	-0.00317	0.0014	-1.66148	-0.00631	0.00496	0.00024	0.00019	57.31165	1.04028	368.51	6.05
5000	0.868	56.39776	0.94658	-0.00114	0.00281	-0.00435	0.00152	-2.27842	-0.00209	0.00516	0.00001	0.00019	57.65231	1.05711	370.49	6.14
6000	0.9417	57.254	1.17833	-0.00044	0.00087	0.00125	0.00055	0.64499	-0.0008	0.00159	0.00019	0.0001	56.8552	1.18576	365.85	6.91
9000	1	56.55824	1.11807	0.00008	0.0013	0.00098	0.0006	0.51235	0.00015	0.00239	0.00029	0.00007	56.23892	1.12931	362.26	6.59
Integrated		67.8603	0.53952	-0.00005	0.00024	0.01376	0.00018	5.99631	-0.00009	0.00045	0.00028	0.00003	63.76326	0.51388	405.64	3.89

11DW3 MU#L1

Weighted average of J from standards = 3.954e-03 +/- 2.790e-05

Laser Power (mW)	Cumulative 39Ar	40Ar/39Ar measured	+/-	37Ar/39Ar measured	+/-	36Ar/39Ar measured	+/-	% Atmosphe 40Ar	Ca/K	+/-	Cl/K	+/-	40*/39K	+/-	Age (Ma)	+/- (Ma)
500	0.0013	122.56575	3.95984	0.06675	0.03682	0.25573	0.01694	61.6669	0.12248	0.06757	0.00491	0.00235	46.97409	4.89432	307.36	29.45
800	0.0103	85.7798	1.57207	0.01175	0.00566	0.09428	0.00359	32.48722	0.02156	0.01039	0.00134	0.00029	57.89276	1.61201	371.88	9.36
1200	0.6131	60.97154	0.82218	0.00049	0.00011	0.00973	0.00015	4.71692	0.00091	0.0002	0.00032	0.00004	58.06729	0.78765	372.9	4.57
1500	0.9237	57.76321	0.79696	0.00045	0.00018	0.00267	0.0001	1.36505	0.00082	0.00033	0.0003	0.00004	56.94543	0.7876	366.38	4.59
2000	0.9561	55.95238	1.07508	0.00253	0.00156	0.00149	0.001	0.78726	0.00465	0.00287	0.00054	0.00014	55.48252	1.11038	357.84	6.5
2500	0.9908	56.48027	1.13465	0.00229	0.00156	0.00134	0.00073	0.7017	0.0042	0.00287	0.00033	0.00011	56.05455	1.15087	361.18	6.72
3000	0.9959	57.10723	0.88499	0.00958	0.01116	0.00035	0.00454	0.18132	0.01758	0.02047	0.0013	0.00067	56.97442	1.60553	366.55	9.35
5000	0.9975	58.64095	2.07569	0.04121	0.03043	0.00686	0.01698	3.45144	0.07563	0.05584	0.00439	0.00216	56.58996	5.41291	364.31	31.55
9000	1	56.32898	1.03039	0.0408	0.01839	-0.00632	0.01019	-3.32385	0.07486	0.03375	0.00181	0.00156	58.17226	3.18645	373.51	18.48
Integrated		59.92385	0.55384	0.00101	0.00016	0.00796	0.00011	3.92736	0.00185	0.00029	0.00035	0.00003	57.54193	0.535	369.85	3.9

11DW7A MU#L1

Weighted average of J from standards = 3.954e-03 +/- 2.790e-05

Laser Power (mW)	Cumulative 39Ar	40Ar/39Ar measured	+/-	37Ar/39Ar measured	+/-	36Ar/39Ar measured	+/-	% Atmosphe 40Ar	Ca/K	+/-	Cl/K	+/-	40*/39K	+/-	Age (Ma)	+/- (Ma)
500	0.0001	309.76975	80.54735	0.16531	0.2027	1.08404	0.34046	103.41601	0.30335	0.37202	-0.00481	0.03252	-10.582	61.79558	-77.11	460.08
800	0.0005	143.81412	8.31221	0.03172	0.05609	0.3813	0.03668	78.36073	0.05821	0.10293	0.00174	0.00446	31.11459	9.96165	209.33	63.28
1200	0.0012	98.84599	3.99152	0.13441	0.02895	0.2364	0.02099	70.68266	0.24665	0.05312	0.00537	0.00267	28.97306	6.30353	195.68	40.35
1500	0.0022	71.69998	2.28609	0.05948	0.01553	0.08803	0.01771	36.29032	0.10914	0.0285	0.00386	0.00179	45.66283	5.55501	299.46	33.57
2000	0.0098	59.63515	0.82167	0.0068	0.00145	0.03927	0.00201	19.46821	0.01247	0.00267	0.00062	0.0004	48.00157	0.95326	313.53	5.72
2500	0.0223	75.56537	1.36882	0.00438	0.0011	0.08817	0.00226	34.49303	0.00804	0.00202	0.00019	0.00029	49.48128	1.33098	322.38	7.94
3000	0.1425	51.51422	0.85984	0.00123	0.00019	0.00996	0.00023	5.71815	0.00225	0.00036	0.00024	0.00005	48.5406	0.82553	316.76	4.94
5000	0.4392	49.95314	0.75579	0.00062	0.00003	0.00364	0.00011	2.15611	0.00114	0.00006	0.00023	0.00004	48.84706	0.74524	318.6	4.46
9000	1	49.50523	0.67932	0.00048	0.00005	0.00121	0.00006	0.72274	0.00088	0.00009	0.00025	0.00004	49.11797	0.67653	320.22	4.04
Integrated		50.39999	0.45817	0.00089	0.00006	0.00486	0.00007	2.85216	0.00163	0.0001	0.00025	0.00003	48.93368	0.45021	319.11	3.39

11DW300A MU#L1

Weighted average of J from standards = 3.954e-03 +/- 2.790e-05

Laser Power (mW)	Cumulative 39Ar	40Ar/39Ar measured	+/-	37Ar/39Ar measured	+/-	36Ar/39Ar measured	+/-	% Atmosphe 40Ar	Ca/K	+/-	Cl/K	+/-	40*/39K	+/-	Age (Ma)	+/- (Ma)
500	0.0014	212.9509	3.0183	0.01146	0.00488	0.56771	0.00682	78.78784	0.02103	0.00896	0.00223	0.0006	45.16556	2.41213	296.45	14.6
800	0.0033	64.43409	0.64917	0.01533	0.00385	0.04705	0.00278	21.58698	0.02813	0.00707	0.00087	0.00036	50.50197	0.97625	328.46	5.81
1200	0.0157	57.13269	0.64865	0.00111	0.00073	0.01423	0.00046	7.36334	0.00204	0.00134	0.00038	0.00007	52.89834	0.6246	342.66	3.68
1500	0.045	52.63362	0.77888	0.00044	0.00031	0.00199	0.00021	1.1193	0.00081	0.00057	0.00024	0.00005	52.01514	0.77359	337.44	4.58
2000	0.1203	52.25088	0.71659	0.00021	0.00013	0.00151	0.00008	0.85288	0.00039	0.00025	0.00027	0.00003	51.7758	0.71176	336.02	4.21
2500	0.275	52.69665	0.62566	0.00008	0.00007	0.00137	0.00007	0.76666	0.00015	0.00013	0.00027	0.00004	52.26317	0.6221	338.91	3.68
3000	0.5078	53.00975	0.54467	-0.00001	0.00006	0.00173	0.00006	0.96349	-0.00003	0.00011	0.00023	0.00003	52.46959	0.54098	340.13	3.2
5000	0.9097	52.64638	0.59675	-0.00005	0.00005	0.00074	0.00003	0.41791	-0.00009	0.00009	0.00024	0.00003	52.39679	0.59485	339.7	3.52
9000	1	52.06072	0.66047	0.00025	0.00011	0.00058	0.00009	0.33163	0.00045	0.0002	0.00024	0.00004	51.85848	0.65913	336.51	3.9
Integrated		52.95709	0.3013	0.0001	0.00003	0.00219	0.00003	1.22498	0.00018	0.00006	0.00025	0.00002	52.27905	0.29848	339	2.81

11DW301A MU#L1

Weighted average of J from standards = 3.954e-03 +/- 2.790e-05

Laser Power (mW)	Cumulative 39Ar	40Ar/39Ar measured	+/-	37Ar/39Ar measured	+/-	36Ar/39Ar measured	+/-	% Atmosphe 40Ar	Ca/K	+/-	Cl/K	+/-	40*/39K	+/-	Age (Ma)	+/- (Ma)
500	0.0005	76.6273	5.83022	-0.0131	0.0437	0.14962	0.03017	57.72079	-0.02403	0.08017	0.00258	0.00438	32.38456	9.79227	217.38	61.93
800	0.002	59.19907	1.37987	0.01501	0.02103	0.04516	0.00438	22.55026	0.02754	0.0386	0.00149	0.00092	45.82701	1.8128	300.45	10.95
1200	0.008	52.14356	0.71621	0.00618	0.00371	0.01546	0.00203	8.76751	0.01133	0.00681	0.00037	0.00024	47.54498	0.90005	310.79	5.4
1500	0.0098	51.34617	1.06861	-0.00971	0.0104	0.00075	0.00395	0.43213	-0.01782	0.01908	0.00039	0.0007	51.09437	1.58084	331.98	9.38
2000	0.0179	48.094	0.72494	0.00057	0.00302	0.00604	0.00084	3.71628	0.00104	0.00555	0.00028	0.00017	46.27811	0.7517	303.17	4.53
2500	0.1125	47.42042	0.64877	0.00087	0.00023	0.00597	0.00023	3.72463	0.00159	0.00042	0.00026	0.00004	45.62562	0.63147	299.23	3.82
3000	0.1614	45.48856	0.63251	0.0004	0.00038	0.0044	0.00025	2.86324	0.00074	0.0007	0.0002	0.00006	44.15728	0.62137	290.34	3.77
5000	0.828	45.6485	0.47315	0.00009	0.00004	0.00205	0.00005	1.33043	0.00017	0.00008	0.00024	0.00003	45.01187	0.46862	295.52	2.84
9000	1	44.58463	0.58232	0.00011	0.00024	0.00071	0.00009	0.47409	0.0002	0.00044	0.00029	0.00004	44.3437	0.58054	291.47	3.52

Integrated		45.72963	0.3388	0.00022	0.00008	0.00255	0.00005	1.65176	0.00041	0.00015	0.00025	0.00002	44.94508	0.33482	295.12	2.79

11DW302B MU#L1

Weighted average of J from standards = 3.954e-03 +/- 2.790e-05

Laser Power (mW)	Cumulative 39Ar	40Ar/39Ar measured	+/-	37Ar/39Ar measured	+/-	36Ar/39Ar measured	+/-	% Atmosphe 40Ar	Ca/K	+/-	Cl/K	+/-	40*/39K	+/-	Age (Ma)	+/- (Ma)
500	0.0031	179.36257	2.28304	0.0282	0.01041	0.46001	0.00939	75.79862	0.05175	0.0191	0.00438	0.00106	43.40189	2.63555	285.74	16.05
800	0.0104	56.03656	0.59174	0.01204	0.00333	0.05838	0.0027	30.79919	0.0221	0.00612	0.00176	0.0003	38.75753	0.93237	257.24	5.77
1200	0.1203	37.82045	0.52557	0.00105	0.00026	0.00202	0.00023	1.57699	0.00193	0.00047	0.00032	0.00005	37.19482	0.52312	247.55	3.25
1500	0.2071	39.43353	0.53998	0.00109	0.00029	0.00872	0.00026	6.54127	0.002	0.00054	0.00032	0.00008	36.82635	0.51602	245.26	3.21
2000	0.2565	43.13804	0.89392	0.00158	0.00046	0.01899	0.00059	13.02004	0.0029	0.00084	0.00027	0.00013	37.49565	0.84901	249.42	5.27
2500	0.6236	39.61562	0.54223	0.00031	0.00008	0.00562	0.00011	4.19524	0.00056	0.00014	0.00027	0.00005	37.9252	0.52421	252.09	3.25
3000	0.758	38.86411	0.54478	0.00072	0.00031	0.00354	0.00017	2.69562	0.00132	0.00058	0.00035	0.00004	37.7876	0.5347	251.23	3.32
5000	0.9352	38.57753	0.59007	0.00041	0.00015	0.00276	0.00013	2.11372	0.00075	0.00027	0.00031	0.00005	37.73305	0.58048	250.89	3.6
9000	1	38.05545	0.68653	0.00104	0.00037	0.00113	0.00032	0.88087	0.00191	0.00069	0.00032	0.00007	37.69082	0.68756	250.63	4.27
Integrated		39.73871	0.25827	0.00081	0.00009	0.00686	0.00008	5.10108	0.00149	0.00016	0.00033	0.00002	37.68345	0.24832	250.58	2.26

11DW303A MU#L1

Weighted average of J from standards = 3.954e-03 +/- 2.790e-05

Laser Power (mW)	Cumulative 39Ar	40Ar/39Ar measured	+/-	37Ar/39Ar measured	+/-	36Ar/39Ar measured	+/-	% Atmosphe 40Ar	Ca/K	+/-	Cl/K	+/-	40*/39K	+/-	Age (Ma)	+/- (Ma)
500	0.0008	103.50037	3.1061	0.03905	0.01976	0.22032	0.01943	62.91811	0.07166	0.03625	0.00468	0.00264	38.36994	5.72843	254.84	35.48
800	0.003	49.87633	0.74907	0.00793	0.00779	0.02958	0.00563	17.53381	0.01456	0.01429	0.0006	0.00085	41.10685	1.79184	271.72	11
1200	0.009	63.20131	1.13752	0.00408	0.00351	0.06761	0.00273	31.6233	0.00749	0.00645	0.00008	0.00027	43.19478	1.19241	284.48	7.27
1500	0.0138	47.13525	0.73106	0.00027	0.00351	0.01232	0.0026	7.72767	0.0005	0.00644	-0.0001	0.00039	43.4654	1.03446	286.13	6.3
2000	0.3902	46.14622	0.58587	0.00005	0.00007	0.00248	0.00007	1.58738	0.00009	0.00013	0.00025	0.00004	45.38447	0.57842	297.77	3.5
2500	0.5813	46.10312	0.60291	0.00029	0.00012	0.00582	0.00014	3.73431	0.00052	0.00022	0.00023	0.00004	44.3529	0.58511	291.52	3.55
3000	0.7644	45.13633	0.61732	0.00016	0.00011	0.00285	0.0001	1.86679	0.0003	0.0002	0.00023	0.00004	44.26459	0.60802	290.99	3.69
5000	0.9727	45.06066	0.62198	0.00012	0.00013	0.0013	0.00012	0.8506	0.00022	0.00023	0.00024	0.00004	44.64793	0.61847	293.31	3.75
9000	1	44.94832	0.84696	0.00056	0.00064	0.00132	0.0005	0.86499	0.00103	0.00117	0.00007	0.00006	44.53009	0.85603	292.6	5.19
Integrated		45.85405	0.30378	0.00022	0.00006	0.00357	0.00006	2.30508	0.0004	0.00011	0.00024	0.00002	44.76807	0.29833	294.04	2.63

11DW304A MU#L1

Weighted average of J from standards = 3.954e-03 +/- 2.790e-05

Laser Power (mW)	Cumulative 39Ar	40Ar/39Ar measured	+/-	37Ar/39Ar measured	+/-	36Ar/39Ar measured	+/-	% Atmosphe 40Ar	Ca/K	+/-	Cl/K	+/-	40*/39K	+/-	Age (Ma)	+/- (Ma)
500	0.0001	170.55879	13.25358	0.07692	0.04781	0.50215	0.04405	87.01035	0.14114	0.08774	0.01388	0.00693	22.15234	8.42866	151.49	55.28
800	0.0006	119.48841	2.71193	0.01919	0.01581	0.26653	0.01113	65.92882	0.03521	0.02901	0.00603	0.00215	40.70154	3.17627	269.23	19.52
1200	0.0028	76.15235	1.06401	0.00772	0.00347	0.12376	0.0027	48.04058	0.01416	0.00637	0.00134	0.00043	39.5531	1.06023	262.16	6.54
1500	0.0146	65.04845	0.88396	0.00249	0.00099	0.08907	0.00134	40.48059	0.00457	0.00181	0.0005	0.00012	38.69884	0.63381	256.88	3.92

2000	0.0891	51.01469	0.69298	0.0007	0.00012	0.04219	0.00067	24.45235	0.00128	0.00021	0.00027	0.00004	38.51798	0.56516	255.76	3.5
2500	0.3628	41.79937	0.47421	0.0002	0.00005	0.01116	0.00013	7.89814	0.00037	0.00009	0.00028	0.00003	38.47065	0.4456	255.47	2.76
3000	0.5816	39.37701	0.46543	0.00025	0.00004	0.00436	0.00009	3.2779	0.00046	0.00007	0.00026	0.00003	38.05755	0.45381	252.91	2.81
5000	0.908	38.73096	0.43137	0.00065	0.00005	0.00284	0.00005	2.17061	0.0012	0.0001	0.00026	0.00003	37.86122	0.42433	251.69	2.63
9000	1	32.11845	0.44321	0.00424	0.0001	0.00077	0.00009	0.70358	0.00779	0.00018	0.00026	0.00004	31.86308	0.44129	214.08	2.8
Integrated		40.46843	0.22905	0.00083	0.00003	0.00967	0.00007	7.06762	0.00152	0.00006	0.00027	0.00002	37.58069	0.21669	249.95	2.13

11DW305A MU#L1

Weighted average of J from standards = 3.954e-03 +/- 2.790e-05

Laser Power (mW)	Cumulative 39Ar	40Ar/39Ar measured	+/-	37Ar/39Ar measured	+/-	36Ar/39Ar measured	+/-	% Atmosphe 40Ar	Ca/K	+/-	Cl/K	+/-	40*/39K	+/-	Age (Ma)	+/- (Ma)
500	0.0024	52.07353	1.24068	0.01103	0.01332	0.06535	0.00859	37.10374	0.02024	0.02444	0.00158	0.00177	32.73388	2.771	219.59	17.5
800	0.0157	47.72986	0.61922	0.0068	0.00155	0.0253	0.00108	15.6716	0.01248	0.00284	0.00056	0.00024	40.22498	0.64174	266.3	3.95
1200	0.0974	41.10513	0.60144	0.00119	0.00035	0.00575	0.00024	4.13883	0.00218	0.00064	0.00024	0.00007	39.37543	0.5869	261.06	3.62
1500	0.162	39.63791	0.52777	0.00088	0.00055	0.00271	0.00031	2.0236	0.00162	0.001	0.00021	0.00008	38.80672	0.52813	257.55	3.27
2000	0.1871	40.08606	0.62852	0.00084	0.00101	0.00503	0.00065	3.7141	0.00155	0.00185	0.00011	0.00014	38.56865	0.64374	256.07	3.98
2500	0.3196	41.75439	0.59467	0.00091	0.00021	0.00719	0.00017	5.09303	0.00168	0.00038	0.00029	0.00007	39.59967	0.57421	262.44	3.54
3000	0.5207	40.32466	0.55488	0.00067	0.00017	0.00423	0.00014	3.10124	0.00122	0.00032	0.00027	0.00004	39.04533	0.54397	259.02	3.36
5000	0.8475	42.80026	0.62539	0.00041	0.00011	0.01216	0.00018	8.39966	0.00076	0.00021	0.00028	0.00005	39.17799	0.58721	259.84	3.63
9000	1	39.5183	0.5768	0.00042	0.00015	0.00143	0.00017	1.06958	0.00077	0.00027	0.00024	0.00005	39.06625	0.57441	259.15	3.55
Integrated		41.34041	0.26641	0.00075	0.00009	0.00726	0.00008	5.19354	0.00137	0.00016	0.00027	0.00002	39.16524	0.25704	259.76	2.33

11DW309A MU#L1

Weighted average of J from standards = 3.954e-03 +/- 2.790e-05

Laser Power (mW)	Cumulative 39Ar	40Ar/39Ar measured	+/-	37Ar/39Ar measured	+/-	36Ar/39Ar measured	+/-	% Atmosphe 40Ar	Ca/K	+/-	Cl/K	+/-	40*/39K	+/-	Age (Ma)	+/- (Ma)
500	0.0007	87.06864	3.47243	0.06025	0.02122	0.21366	0.01748	72.53415	0.11056	0.03894	0.00442	0.003	23.907	5.11362	162.96	33.33
800	0.0015	62.44124	2.58621	0.01738	0.02018	0.08753	0.0141	41.44191	0.03189	0.03703	0.00334	0.00164	36.54745	4.57481	243.52	28.51
1200	0.0041	55.42035	0.94369	0.01317	0.00642	0.04839	0.00395	25.81139	0.02417	0.01178	0.00106	0.00049	41.09393	1.36838	271.64	8.4
1500	0.0091	44.3896	0.61036	-0.00056	0.00242	0.01074	0.00186	7.15318	-0.00104	0.00443	0.00039	0.00026	41.18674	0.79958	272.21	4.91
2000	0.0745	41.06883	0.5651	0.0004	0.00021	0.00212	0.00018	1.52512	0.00074	0.00038	0.00029	0.00004	40.41325	0.55995	267.45	3.44
2500	0.3849	40.55612	0.52085	0.0001	0.00005	0.00102	0.00004	0.74717	0.00018	0.00009	0.00024	0.00004	40.22362	0.51766	266.29	3.19
3000	0.7502	41.28248	0.49449	0.00007	0.00005	0.00072	0.00004	0.51632	0.00013	0.00009	0.00028	0.00004	41.03979	0.49247	271.3	3.02
5000	0.9728	40.42491	0.53202	0.00015	0.00008	0.00033	0.00007	0.23808	0.00028	0.00015	0.00029	0.00004	40.29904	0.53137	266.75	3.27
9000	1	40.09145	0.69715	-0.00051	0.00041	0.00041	0.00041	0.30168	-0.00093	0.00075	0.00023	0.00007	39.94088	0.70684	264.55	4.35
Integrated		40.92059	0.27342	0.00019	0.00005	0.0012	0.00004	0.8677	0.00035	0.00008	0.00028	0.00002	40.53609	0.27162	268.21	2.43

12DW1A MU#L1

Weighted average of J from standards = 3.954e-03 +/- 2.790e-05

Laser Power	Cumulative	40Ar/39Ar	+/-	37Ar/39Ar	+/-	36Ar/39Ar	+/-	% Atmosphe	Ca/K	+/-	Cl/K	+/-	40*/39K	+/-	Age	+/-

(mW)	39Ar	measured		measured		measured		40Ar							(Ma)	(Ma)
500	0	576.26309	2927.4062	7.31763	37.12994	0.64602	4.39494	33.02411	13.4966	68.83798	0.61445	3.14189	387.94234	2191.4305	1677.43	6169.3
800	0	-605.6418	1525.7312	-2.77168	7.44035	-0.98274	2.8624	47.90912	-5.07573	13.59874	-0.13096	0.42774	-314.8833	922.34604	-8089.68	26844
1200	0.0008	77.02061	22.56771	0.18294	0.1792	0.10295	0.1076	39.49243	0.33571	0.3289	0.00433	0.02178	46.59135	37.23017	305.06	224.27
1500	0.0022	25.44624	12.03793	0.03235	0.11436	-0.1014	0.07823	-117.8959	0.05936	0.20984	0.01666	0.01314	55.38286	26.40065	357.26	154.5
2000	0.0427	25.1626	0.39774	0.00515	0.00476	0.03179	0.00319	37.37035	0.00945	0.00873	0.00057	0.00054	15.74071	0.99428	108.93	6.68
2500	0.2328	15.77689	0.21907	0.00059	0.00101	0.00194	0.00051	3.64824	0.00108	0.00186	0.00031	0.0001	15.1727	0.26173	105.11	1.76
3000	0.6259	15.33565	0.27285	0.00065	0.0005	0.00039	0.00032	0.75109	0.00119	0.00091	0.0003	0.00007	15.191	0.28809	105.24	1.94
5000	0.9184	17.08465	0.28505	0.00037	0.00052	0.00623	0.00039	10.78926	0.00068	0.00096	0.00036	0.00012	15.21485	0.29227	105.4	1.97
9000	1	15.59991	0.21495	0.00339	0.00229	0.00119	0.00156	2.26151	0.00622	0.0042	0.00057	0.00024	15.21813	0.50677	105.42	3.41
Integrated		16.48444	0.15021	0.00163	0.00054	0.00378	0.00034	6.78756	0.003	0.001	0.00041	0.00007	15.33788	0.17579	106.23	1.39

12DW3D MU#L1

Weighted average of J from standards = 3.954e-03 +/- 2.790e-05

Laser Power (mW)	Cumulative 39Ar	40Ar/39Ar measured	+/-	37Ar/39Ar measured	+/-	36Ar/39Ar measured	+/-	% Atmosphe 40Ar	Ca/K	+/-	Cl/K	+/-	40*/39K	+/-	Age (Ma)	+/- (Ma)
500	0.0057	43.77509	0.59572	0.01599	0.00555	0.12916	0.00639	87.24789	0.02933	0.01018	0.00281	0.00095	5.57852	1.85477	39.36	12.95
800	0.0187	24.5285	0.29666	-0.00155	0.00144	0.03352	0.0019	40.43047	-0.00284	0.00264	0.00004	0.00023	14.5938	0.59384	101.21	4.01
1200	0.0974	15.64624	0.29242	0.00032	0.00036	0.00497	0.00034	9.39802	0.00058	0.00066	0.0002	0.00008	14.1489	0.29471	98.21	1.99
1500	0.3314	13.82665	0.19459	0.00037	0.00011	0.00048	0.00012	1.03831	0.00068	0.0002	0.00023	0.00004	13.6537	0.19614	94.86	1.33
2000	0.6031	13.86376	0.18098	0.00017	0.0001	0.00029	0.0001	0.62155	0.00031	0.00017	0.00021	0.00004	13.74808	0.18262	95.5	1.24
2500	0.7524	13.80023	0.26667	-0.00022	0.0002	0.00012	0.0001	0.26255	-0.00039	0.00037	0.00024	0.00007	13.73437	0.26809	95.41	1.81
3000	0.8135	13.83793	0.22748	-0.00043	0.00034	0.00011	0.00038	0.23966	-0.00079	0.00062	0.00016	0.00009	13.77513	0.25322	95.68	1.71
5000	0.8612	13.88177	0.21568	-0.00105	0.00061	-0.00023	0.00037	-0.48964	-0.00192	0.00113	0.00017	0.00008	13.91988	0.24205	96.66	1.64
9000	1	13.83187	0.27666	-0.0001	0.00032	0.00009	0.00016	0.18231	-0.00017	0.00058	0.00022	0.00007	13.777	0.28044	95.7	1.9
Integrated		14.29092	0.0934	0.00011	0.00009	0.00179	0.00008	3.70066	0.0002	0.00016	0.00023	0.00002	13.73346	0.09362	95.4	0.91

12DW60A MU#L1

Weighted average of J from standards = 3.954e-03 +/- 2.790e-05

Laser Power (mW)	Cumulative 39Ar	40Ar/39Ar measured	+/-	37Ar/39Ar measured	+/-	36Ar/39Ar measured	+/-	% Atmosphe 40Ar	Ca/K	+/-	Cl/K	+/-	40*/39K	+/-	Age (Ma)	+/- (Ma)
500	0.0008	156.04104	21.21151	-0.09593	0.18266	0.3386	0.11337	64.13891	-0.176	0.33512	0.01292	0.01175	55.94358	33.13224	360.53	193.54
800	0.0024	100.47983	8.5832	-0.04678	0.091	0.12574	0.06633	36.99241	-0.08584	0.16697	0.00768	0.00743	63.28912	20.55675	402.94	117.29
1200	0.0133	58.2742	0.921	0.00553	0.01304	0.03342	0.01103	16.95299	0.01015	0.02392	0.0012	0.00097	48.3705	3.35701	315.75	20.1
1500	0.034	67.31767	1.06924	0.00262	0.00945	0.0656	0.00444	28.80822	0.0048	0.01734	0.00137	0.00078	47.90359	1.55871	312.95	9.35
2000	0.1908	49.54429	1.02238	-0.00038	0.00101	0.00948	0.00068	5.6581	-0.0007	0.00185	0.00031	0.0001	46.713	1.01318	305.79	6.1
2500	0.6497	47.10102	0.70159	0.00033	0.00038	0.00283	0.00026	1.77794	0.0006	0.0007	0.0003	0.00006	46.23443	0.6954	302.91	4.19
3000	0.7081	47.07718	0.80639	-0.00074	0.00234	0.00074	0.0016	0.4626	-0.00137	0.00429	0.0004	0.00021	46.82981	0.93241	306.5	5.61
5000	0.9996	46.76923	0.62835	0.00039	0.00054	0.00199	0.00034	1.25559	0.00071	0.00098	0.00036	0.00007	46.15268	0.63003	302.42	3.8
9000	1	60.08067	38.87204	-0.79015	0.60676	-0.39395	0.33189	-193.7495	-1.44901	1.11209	-0.02667	0.03912	176.30096	121.34645	954.25	510.07
Integrated		48.10508	0.41296	-0.00016	0.00048	0.00547	0.00031	3.36323	-0.00029	0.00087	0.00037	0.00005	46.45849	0.41211	304.26	3.17

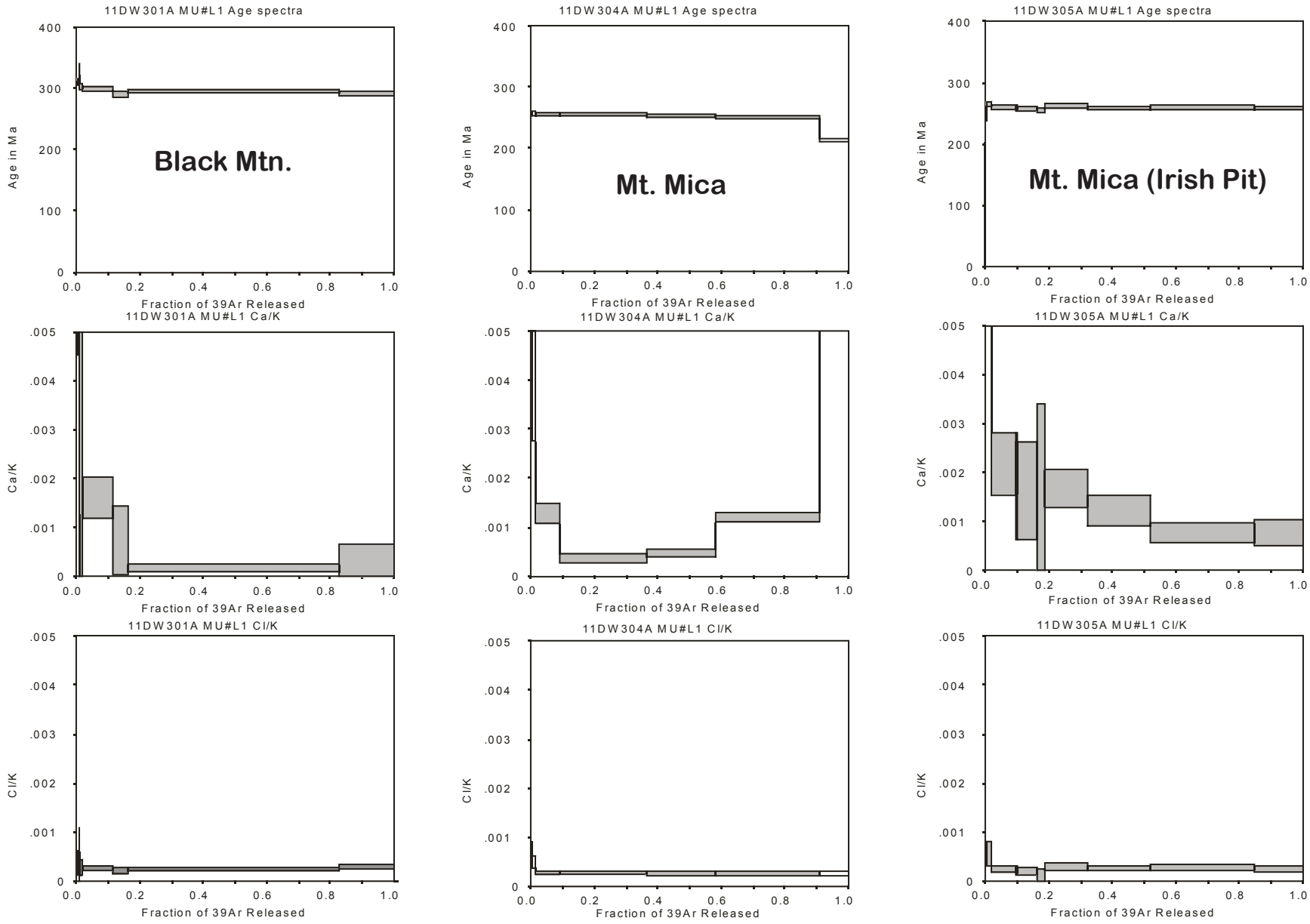

Fig. B1, Bradley et al, New England pegmatite geochronology—Appendix B
Sheet 1 of 4

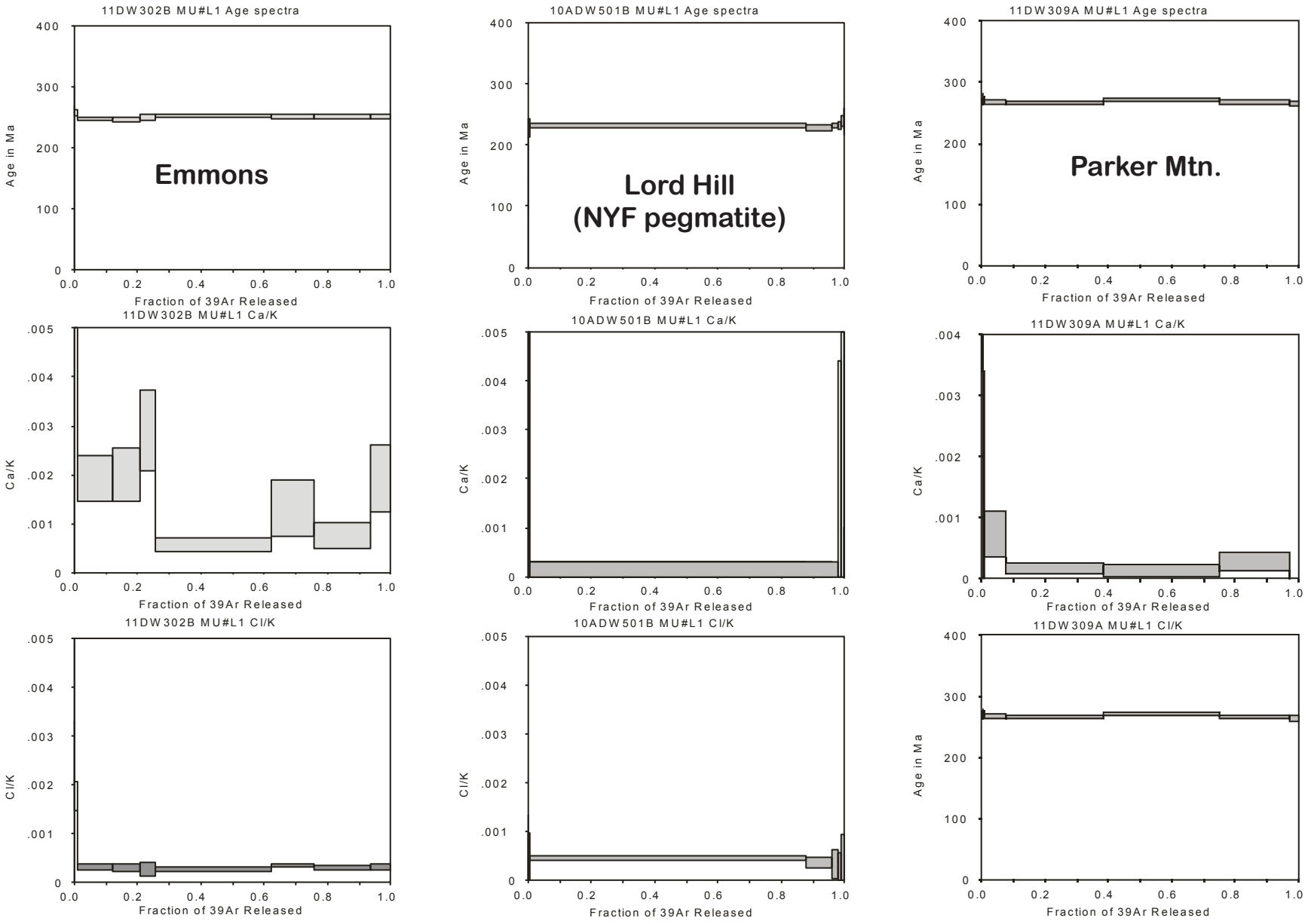

Fig. B1, Bradley et al, New England pegmatite geochronology—Appendix B
Sheet 2 of 4

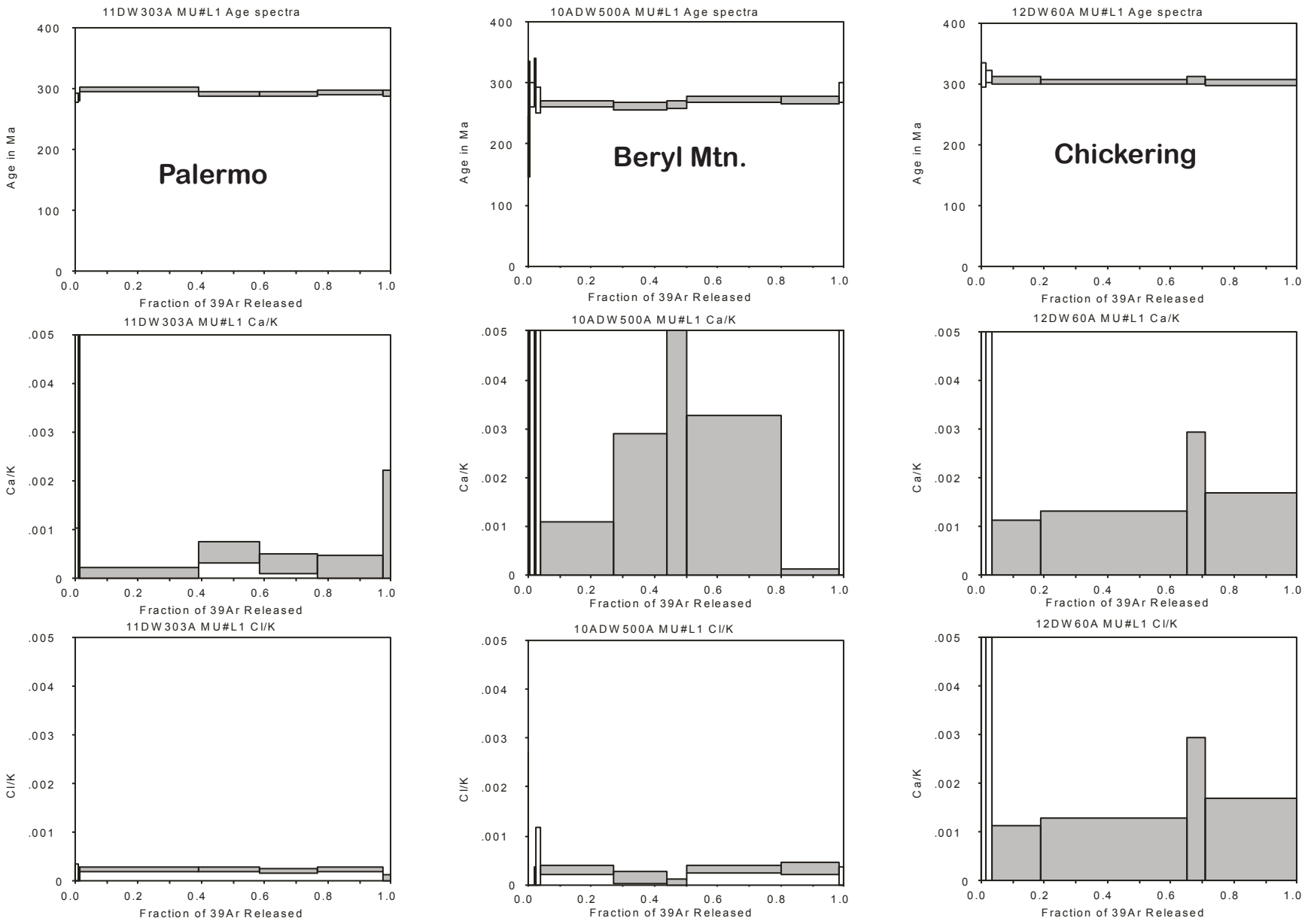

Fig. B1, Bradley et al, New England pegmatite geochronology—Appendix B
Sheet 3 of 4

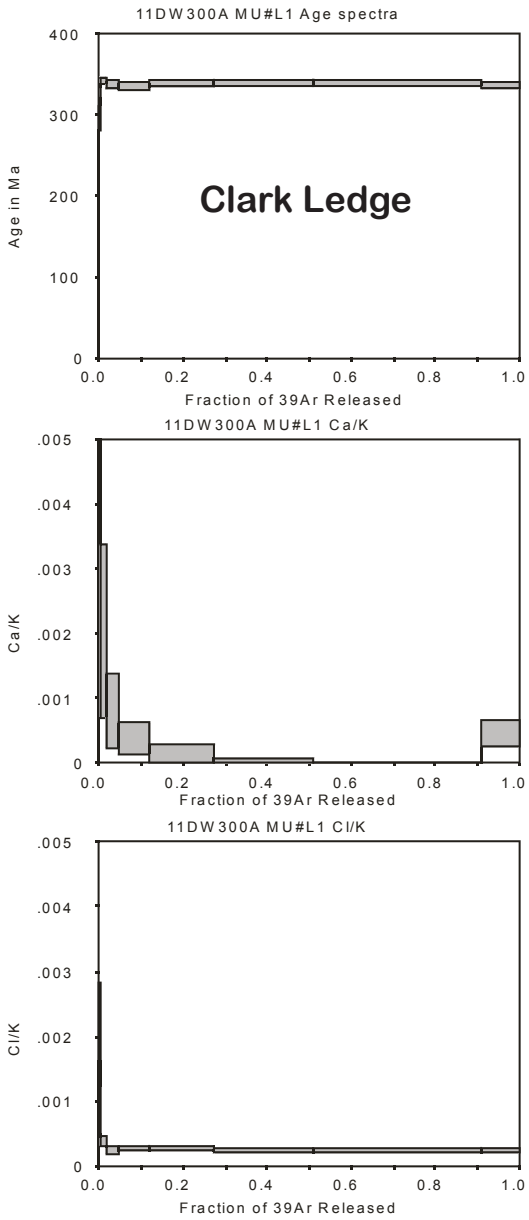

Fig. B1, Bradley et al, New England pegmatite geochronology—Appendix B
Sheet 4 of 4

APPENDIX C (APATITE)

ANALYTICAL METHODS—Apatite Thermochronology and Geochronology by Apatite to Zircon, Inc.

Sample Preparation

Sample preparation methods used here were presented in detail by Donelick et al. (2005). Fission tracks were viewed and counted or measured at 2000x (Zeiss Axioplan microscope; analyst Paul O'Sullivan) dry magnification using unpolarized, transmitted light with or without reflected light. All AFT age and AFT length grains were selected to sample the greatest range of observable characteristics (size, degree of roundness, color, etch figure size, etc.).

LA-ICP-MS Session Details

Data were collected for the isotopes listed in Table C1. The data acquisition parameters for the laser ablation system and mass spectrometer are listed in Table C2.

General ICP-MS Data Modeling

Terms used in this discussion are tabulated and defined below. Steps for calculating background intensity for an isotope at a spot were as follow:

1. The final background scan was assigned as the last scan for which ^{43}Ca and ^{232}Th intensities were near their respective minima prior to systematically increasing (if ^{43}Ca and ^{232}Th exhibit no such minima, the analysis was deemed a failure; failure is usually due to loss of the grain after being dislodged by the laser or the grain may have been inaccessible to the laser within the sample cell during the LA-ICP-MS session). The first signal scan followed a fixed number of scans (the number fixed session-wide) after the final background scan (first signal scan is number 18 for the spot in Figure C1, 5 scans after the final background scan).
2. A line was fitted to the scan background intensities for individual isotopes, B_{scan} values, (scans 1-13 in Figure C1) by chi-squared minimization, outliers identified, and a line again fitted to B_{scan} values excluding the outliers.
3. For a fitted line exhibiting a negative slope (corresponding to decreasing B_{scan} values through time), the value of the fitted line at the first signal scan was assigned as the spot background intensity B_{spot}. For a fitted line exhibiting a zero or positive slope, the mean of B_{scan} values excluding the outliers was assigned as B_{spot}.

Steps for session-wide smoothing of background were as follow (Figure C2):

1. The session-wide trend of B_{spot} for each isotope was smoothed using a moving window of spots (*max* in Table C1 for isotopes requiring significant smoothing; *min* in Table C1 for isotopes requiring retention of significant and/or sharp structure).
2. For each isotope at each session spot, the window of spots was positioned with the spot of interest at the right-hand-side of the window and a line was fitted to all B_{spot} values within the window (with outliers removed using a two-regression process). For windows extending left of spot 1 in the session, all $B_{spot<1}$ were set equal to $B_{spot=1}$. Similarly, for windows extending right of the last spot in the session, all $B_{spot>last}$ were set equal to $B_{spot=last}$. The fitted line was evaluated at the spot of interest giving B_{spot_window}; σ_{Bspot_window} was evaluated as the standard deviation of B_{spot} values within the window about the fitted line.
3. The window was shifted one spot to the right and the process was repeated until the spot of interest was positioned at the left-hand-side of the window. The number of B_{spot_window} and σ_{Bspot_window} values for the spot of interest equaled the number of scans defining the width of the window.
4. The session-wide, smoothed background intensity B_{spot_smooth} for the spot of interest was taken as the median of the B_{spot_window} values from all positions of the moving window.
5. The session-wide, smoothed standard deviation of the background intensity σ_{Bspot_smooth} for the spot of interest was taken as the median of the σ_{Bspot_window} values from all positions of the moving window.

Steps for calculating background error at a spot were as follow:

1. For $B_{spot} \leq B_{spot\_smooth} + 2\sigma_{Bspot\_smooth}$, σ_{Bspot_smooth} was left unchanged.
2. For $B_{spot} > B_{spot\_smooth} + 2\sigma_{Bspot\_smooth}$, σ_{Bspot_smooth} was increased by $0.5*(B_{spot}-B_{spot\_smooth})$.

Steps for calculating smoothed signal at each signal scan at a spot were as follow:

1. Scan raw signal intensities, SB_{scan} values, (scans 18-53 in Figure C1a and Figure 1b) were modeled by fitting a sum of ≤10 Gaussian equations using chi-squared minimization. Two fitting passes were performed: after the first pass, all raw signal values greater than two standard deviations away from the sum of fitted Gaussians were designated outliers; the second pass fit the sum of Gaussians to the data excluding the outliers.
2. Scan background-corrected signal intensity S_{scan} was set equal to $SB_{scan} - B_{spot\_smooth}$.
3. All S_{scan} values for a spot were migrated in time, taking into account the acquisition times and mass differences between successively analyzed isotopes. In the remainder of this paper, scan refers to a integer multiple of the time required to complete a single data collection scan and each S_{scan} value for a given scan represents a migrated value at fixed time.

Steps for calculating smoothed signal error at each signal scan at a spot were as follow:

1. The standard deviation of the non-outlier SB_{scan} values about their respective sum of fitted Gaussians was taken as the absolute signal intensity error σ_{Sscan} for each data scan, the value constant for all scans at a spot.
2. The error for a single isotope at a single scan $\sigma_{isotope}$ was set equal to $(\sigma_{Sscan}^2 + \sigma_{Bspot\_smooth}^2)^{0.5}$.
3. The error of the sum of N S_{scan} values for a particular isotope was taken as the product of $N^{1/2}$ $\sigma_{isotope}$.

Steps for correcting ^{238}U values for detection efficiency variations were as follow:

1. In a session where ^{235}U and ^{238}U raw signals were directly measured, the $^{238}U/^{235}U$ ratio was determined for each data scan at each spot. A regression of ^{238}U signal (abscissa) versus $^{238}U/^{235}U$ ratio (ordinate) was performed for all scans for which ^{238}U exceeds some user-defined value. The results of this regression were presented to the user so that the user could: a) use the resultant regression to correct ^{238}U signals for detection efficiency bias, effectively rendering the $^{238}U/^{235}U$ ratio independent of ^{238}U signal, or b) adjust the user-defined ^{238}U lower limit so that the data could be re-processed and a new regression assessed, or c) ignore the resultant regression and accept the ^{238}U signal values in their uncorrected form.
2. The process described above can, in some cases, permit the user to identify evidence of problems with pulse versus analog detection mode when ^{238}U signal intensities are sufficiently high to cause the detection mode to switch.

AFT Data Analysis

ICP-MS data modeling. Fission track ages were calculated using the scheme presented by Donelick et al. (2005) using a modified zeta calibration approach after Hurford and Green (1983; see also Hasabe et al., 2003). The $^{238}U/^{43}Ca$ ratio for each data scan was calculated using the background-corrected, sum-of-Gaussian-fitted signal values for the two isotopes.

1. Each data scan was treated as a slice of ablated mineral where: a) the thickness of the slice was determined by the S_{scan} value for ^{43}Ca multiplied by a calibration factor in terms of microns per ^{43}Ca, and b) the depth of the slice was determined by the sum of the thicknesses of the overlying slices plus one half of the thickness of the current slice.
2. The S_{scan} value for ^{238}U and the S_{scan} value for ^{43}Ca were used to calculate the $^{238}U/^{43}Ca$ ratio for each slice and a weighted sum for this ratio was calculated by weighting each slice according to: a) slice thickness and b) slice depth converted to the likelihood that fission tracks emanating from that depth could intersect the polished and etched mineral surface. Below $l_o/2$ (l_o taken as the mean length of natural DR tracks), the likelihood of ^{238}U contributing fission tracks to the etched apatite surface is effectively zero.

3. The error of the weighted mean $^{238}U/^{43}Ca$ ratio was calculated as follows:

$$\left(\frac{^{238}U}{^{43}Ca}\right)_{\sigma} = \left(N\left(\frac{\sigma_{isotope\_^{43}Ca}}{\sum ^{43}Ca}\right)^2 + N\left(\frac{\sigma_{isotope\_^{238}U}}{\sum ^{238}U}\right)^2\right)^{1/2}$$

where

$\Sigma^{43}Ca$ = sum of S_{scan} values for ^{43}Ca above a depth of $l_o/2$
$\Sigma^{238}U$ = sum of S_{scan} values for ^{238}U above a depth of $l_o/2$
N = number of scans above a depth of $l_o/2$.

Zeta age standard. DR was used as the apatite FT zeta age calibration standard (Table 3). During each LA-ICP-MS session containing samples of unknown FT age, at least 50 spots of DR apatite (these DR spots corresponding to specific spots from the primary zeta calibration session performed previously) were analyzed during the session for purposes of calibrating $^{238}U/^{43}Ca$. This method is analogous to using ^{235}U-doped glass standards in the external detector method of fission track analysis (Donelick et al., 2005); in this study, specific DR grains from the primary standard LA-ICP-MS session serve as ^{235}U-doped standards.

UPb Data Analysis

UPb ICP-MS data modeling. Previous LA-ICP-MS studies of UPb zircon dating used the so-called intercept method which assumes that isotopic ratio varies linearly with scan number due solely to linearly varying isotopic fractionation (Chang et al., 2006; Gerhels et al., 2008). For the intercept method, a line is fitted to background-corrected isotopic ratio (e.g., $^{206}Pb/^{238}U$) versus data scan number and the intercept of the fitted line (corresponding to data scan number = 0) is used as the isotopic ratio for age calculation and the error on the intercept is used for age error calculation. The data modeling approach here utilized individual S_{scan} and $\sigma_{scan\_isotope}$, the former migrated to constant time for each scan.

UPb standard details. Apatite UPb age standards for which independently accepted ages are published were designated as primary, secondary, and tertiary for purposes of age calibration (Table 3). A minimum of two primary and two secondary standard spots were analyzed prior to and following each group of ~25-40 tertiary standards and/or unknown sample spots. Typically, 5-25 spots of each tertiary standard were analyzed near the beginning and again near the end of each LA-ICP-MS session.

Pb/U fractionation factors. For each primary standard data scan, fractionation factors and their errors, f_{scan} and σ_{fscan} values, were determined based on S_{scan} and $\sigma_{scan\_isotope}$ values for the isotopes of interest using the scheme detailed in Appendix 2. In a process similar to that for smoothing background intensities and their errors, f_{scan_smooth} and σ_{fscan_smooth} values were calculated for every scan at every spot in the LA-ICP-MS session. For each spot in the session, the isotopes of interest were summed over all data scans and used to determine fractionation factors and their errors for each spot, f_{spot} and σ_{fspot}, respectively and these were smoothed to yield session-wide spot fractionation factors and their errors f_{spot_smooth} and σ_{fspot_smooth}. Session-wide smoothing of the fractionation factors was performed using the moving window approach described above where: a) the window width was dynamic, encompassing 15 primary standard spots including primary standard spots at the left- and right-hand-sides and b) the session was divided into independent sub-sessions delineated by session breaks such as sample exchanges, long dormant periods, and gas cylinder exchanges. For a particular isotopic ratio (e.g., $^{206}Pb/^{238}U$), the fractionation factor equals the accepted isotopic ratio divided by the measured ratio. Fractionation factors were calculated based on the following assumptions: a) ^{235}U values were calculated from measured ^{238}U values (Steiger and Jäger, 1977), b) zero fractionation was assumed between ^{206}Pb and ^{207}Pb, and c) the independently measured initial $^{207}Pb/^{206}Pb$ ratio of 0.881984 (Schoene and Bowring, 2006) for McClure Mountain apatite was used. The Stacey and Kramer (1975) common Pb model for Earth was used in this study. Ages and common Pb ratios were determined iteratively using a pre-set, session-wide minimum common Pb age value (the default minimum common Pb age was set equal to the age of the oldest age standard; secondary standard F5 and tertiary standard FC are both 1099.0 Ma and both were the oldest standards analyzed).

Finally, fractionation factors were normalized using the scheme presented in Appendix 3.

UPb ages and age errors. For a single scan, the UPb age t_{scan} and its error σ_{tscan} were calculated as follows:

$$t_{scan} = G_t(S_{scan1}, S_{scan2})$$

$$\sigma_{tscan} = t_{scan} \left(\left(\sigma_{fscan\_smooth} / f_{scan\_smooth} \right)^2 + \left(\sigma_{isotope1} / S_{scan1} \right)^2 + \left(\sigma_{isotope2} / S_{scan2} \right)^2 \right)^{0.5}$$

where:

G_t is a function that returns age t for isotopic values S_{scan1} and S_{scan2}
$\sigma_{isotope1} = \sigma_{isotope}$ for isotope 1
$S_{scan1} = S_{scan}$ for isotope 1
$\sigma_{isotope2} = \sigma_{isotope}$ for isotope 2
$S_{scan2} = S_{scan}$ for isotope 2

For a sum of N scans, the UPb age t_{Nscan} and its error σ_{tNscan} was calculated as follows:

$$t_{Nscan} = G_t(w\Sigma S_{scan1}, w\Sigma S_{scan2})$$

$$\text{for } (\sigma_{fscan\_wm}/N^{0.5}) \geq \sigma_{fspot\_smooth}:$$
$$\sigma_{tNscan} = t_{Nscan} \left(\left((\sigma_{fscan\_wm}/N^{0.5})/f_{scan\_wm}\right)^2 + N(\sigma_{isotope1} / w\Sigma S_{scan1})^{\,2} + N(\sigma_{isotope2} / w\Sigma S_{scan2})^{\,2}\right)^{0.5}$$

$$\text{for } (\sigma_{fscan\_wm}/N^{0.5}) < \sigma_{fspot\_smooth}:$$
$$\sigma_{tNscan} = t_{Nscan} \left((\sigma_{fspot\_smooth}/f_{scan\_wm})^2 + N(\sigma_{isotope1} / w\Sigma S_{scan1})^{\,2} + N(\sigma_{isotope2} / w\Sigma S_{scan2})^{\,2}\right)^{0.5}$$

where:

$w\Sigma S_{scan1}$ = weighted sum of S_{scan1} over N scans, each scan weighted by the parent isotope
$w\Sigma S_{scan2}$ = weighted sum of S_{scan2} over N scans, each scan weighted by the parent isotope
σ_{fscan_wm} = weighted mean σ_{fscan} over N scans, each scan weighted by the parent isotope
f_{scan_wm} = weighted mean f_{scan} over N scans, each scan weighted by the parent isotope

The error σ_{tspot} for the UPb age t_{spot} based on isotopic sums was calculated as follows:

$$\sigma_{tspot} = t_{spot} \left((\sigma_{fspot\_smooth}/f_{spot\_smooth})^2 + N(\sigma_{isotope1} / w\Sigma S_{scan1})^{\,2} + N(\sigma_{isotope2} / w\Sigma S_{scan2})^{\,2}\right)^{0.5}$$

Terms Defined

Background for Individual Isotopes

B_{scan} = scan background intensities
B_{spot} = spot background intensities

B_{spot_window} = smoothed spot background intensity within the moving window; total number of these values equals the number of spot defining the window width

σ_{Bspot_window} = smoothed standard deviation of B_{spot_smooth} within the moving window; total number of these values equals the number of spot defining the window width

B_{spot_smooth} = median of of B_{spot_window} values at a spot of interest

σ_{Bspot_smooth} = median of of σ_{Bspot_window} values at a spot of interest; absolute error of B_{spot_smooth}

Signal for Individual Isotopes

SB_{scan} = scan raw signal intensities

S_{scan} = scan background-corrected signal intensities

σ_{Sscan} = absolute error of S_{scan}; constant for all scans

$\sigma_{isotope}$ = absolute error of isotope at a scan; constant for all scans

Fractionation Factors

$^{206}Pb_m$ = measured ^{206}Pb

$^{207}Pb_m$ = measured ^{207}Pb

$^{206*}Pb$ = radiogenic ^{206}Pb

$^{207*}Pb$ = radiogenic ^{207}Pb

$^{206}Pb_{com}$ = common ^{206}Pb

$^{207}Pb_{com}$ = common ^{207}Pb

$^{238}U_m$ = measured ^{238}U

$^{235}U_m$ = measured ^{235}U (or calculated = $^{238}U_m/137.88$)

f_{207} = fractionation factor for $^{207}Pb_m/^{235}U_m$

f_{206} = fractionation factor for $^{206}Pb_m/^{238}U_m$

f_{Pb}= fractionation factor for $^{207}Pb_m/^{206}Pb_m$

t_{std} = age of standard

137.88 = natural $^{238}U/^{235}U$ ratio

f_{scan} = scan fractionation factor

σ_{fscan} = scan fractionation factor error

f_{scan_smooth} = session-wide, smoothed scan fractionation factor

σ_{fscan_smooth} = session-wide, smoothed scan fractionation factor error
f_{spot} = spot fractionation factor
σ_{fspot}= spot fractionation factor error
f_{spot_smooth} = session-wide, smoothed spot fractionation factor
σ_{fspot_smooth} = session-wide, smoothed spot fractionation factor error

UPb Ages

t_{scan}= UPb age of a single scan
t_{spot} = UPb age of a sum of *N* scans

Fractionation Factors for data Containing Common Terrestrial Pb

Starting equations:

$$\left(\frac{^{207*}Pb}{^{235}U}\right)_{std} = \exp(\lambda_{235U} t_{std}) - 1$$

$$\left(\frac{^{206*}Pb}{^{235}U}\right)_{std} = \exp(\lambda_{238U} t_{std}) - 1$$

$$f_{207} = \frac{\left(\frac{^{207*}Pb}{^{235}U}\right)_{std}}{\left(\frac{^{207*}Pb_m}{^{235}U_m}\right)}$$

$$f_{206} = \frac{\left(\frac{^{206*}Pb}{^{238}U}\right)_{std}}{\left(\frac{^{206*}Pb_m}{^{238}U_m}\right)}$$

$$^{207*}Pb = {}^{207}Pb_m - {}^{206}Pb_{com}\left(\frac{^{207}Pb_{com}}{^{206}Pb_{com}}\right)_{std}$$

$$^{206*}Pb = {}^{206}Pb_m - {}^{206}Pb_{com}$$

Substitute:

$$f_{207} = \frac{\left(\frac{^{207*}Pb}{^{235}U}\right)_{std}}{\left(\frac{^{207}Pb_m - {}^{206}Pb_{com}\left(\frac{^{207}Pb_{com}}{^{206}Pb_{com}}\right)_{std}}{^{235}U_m}\right)} \qquad \text{(A1a)}$$

$$f_{206} = \frac{\left(\frac{^{206*}Pb}{^{238}U}\right)_{std}}{\left(\frac{^{206}Pb_m - {}^{206}Pb_{com}}{^{238}U_m}\right)} \qquad \text{(A1b)}$$

Assume:

$$f_{206} = Rf_{207}$$

because $^{235}U_m$ is usually calculated directly from $^{238}U_m$ and the mass spectrometer detector's registration efficiency ratio $^{207}Pb_m/^{206}Pb_m$ equals R.

For R≠1:

$$\frac{\left(\frac{^{206*}Pb}{^{238}U}\right)_{std}}{\left(\frac{^{206}Pb_m - ^{206}Pb_{com}}{^{238}U_m}\right)} = \frac{R\left(\frac{^{207*}Pb}{^{235}U}\right)_{std}}{\left(\frac{^{207}Pb_m - ^{206}Pb_{com}\left(\frac{^{207}Pb_{com}}{^{206}Pb_{com}}\right)_{std}}{^{235}U_m}\right)}$$

$$\left(\frac{^{206*}Pb}{^{238}U}\right)_{std}\left(\frac{^{207}Pb_m - ^{206}Pb_{com}\left(\frac{^{207}Pb_{com}}{^{206}Pb_{com}}\right)_{std}}{^{235}U_m}\right) = R\left(\frac{^{207*}Pb}{^{235}U}\right)_{std}\left(\frac{^{206}Pb_m - ^{206}Pb_{com}}{^{238}U_m}\right)$$

$$\left(\frac{^{207}Pb_m\left(\frac{^{206*}Pb}{^{238}U}\right)_{std}}{^{235}U_m}\right) - \left(\frac{^{206}Pb_{com}\left(\frac{^{207}Pb_{com}}{^{206}Pb_{com}}\right)_{std}\left(\frac{^{206*}Pb}{^{238}U}\right)_{std}}{^{235}U_m}\right) = \left(\frac{^{206}Pb_m R\left(\frac{^{207*}Pb}{^{235}U}\right)_{std}}{^{238}U_m}\right) - \left(\frac{^{206}Pb_{com}R\left(\frac{^{207*}Pb}{^{235}U}\right)_{std}}{^{238}U_m}\right)$$

$$\left(\frac{{}^{206}Pb_{com}R\left(\frac{{}^{207*}Pb}{{}^{235}U}\right)_{std}}{{}^{238}U_m}\right)-\left(\frac{{}^{206}Pb_{com}\left(\frac{{}^{207}Pb_{com}}{{}^{206}Pb_{com}}\right)_{std}\left(\frac{{}^{206*}Pb}{{}^{238}U}\right)_{std}}{{}^{235}U_m}\right)=\left(\frac{{}^{206}Pb_m R\left(\frac{{}^{207*}Pb}{{}^{235}U}\right)_{std}}{{}^{238}U_m}\right)-\left(\frac{{}^{207}Pb_m\left(\frac{{}^{206*}Pb}{{}^{238}U}\right)_{std}}{{}^{235}U_m}\right)$$

Solve for ${}^{206}Pb_{com}$:

$${}^{206}Pb_{com}=\frac{\frac{R\left({}^{206}Pb_m\left(\frac{{}^{207*}Pb}{{}^{235}U}\right)_{std}\right)}{{}^{238}U_m}-\frac{\left({}^{207}Pb_m\left(\frac{{}^{206*}Pb}{{}^{238}U}\right)_{std}\right)}{{}^{235}U_m}}{\frac{R\left(\frac{{}^{207*}Pb}{{}^{235}U}\right)_{std}}{{}^{238}U_m}-\frac{\left(\left(\frac{{}^{207}Pb_{com}}{{}^{206}Pb_{com}}\right)_{std}\left(\frac{{}^{206*}Pb}{{}^{238}U}\right)_{std}\right)}{{}^{235}U_m}} \qquad \text{(A2a)}$$

For R=1:

$$\frac{\left(\frac{{}^{206*}Pb}{{}^{238}U}\right)_{std}}{\left(\frac{{}^{206}Pb_m-{}^{206}Pb_{com}}{{}^{238}U_m}\right)}=\frac{\left(\frac{{}^{207*}Pb}{{}^{235}U}\right)_{std}}{\left(\frac{{}^{207}Pb_m-{}^{206}Pb_{com}\left(\frac{{}^{207}Pb_{com}}{{}^{206}Pb_{com}}\right)_{std}}{{}^{235}U_m}\right)}$$

$$\left(\frac{^{206*}Pb}{^{238}U}\right)_{std}\left(\frac{^{207}Pb_m - {}^{206}Pb_{com}\left(\frac{^{207}Pb_{com}}{^{206}Pb_{com}}\right)_{std}}{^{235}U_m}\right) = \left(\frac{^{207*}Pb}{^{235}U}\right)_{std}\left(\frac{^{206}Pb_m - {}^{206}Pb_{com}}{^{238}U_m}\right)$$

$$\left(\frac{^{207}Pb_m\left(\frac{^{206*}Pb}{^{238}U}\right)_{std}}{^{235}U_m}\right) - \left(\frac{^{206}Pb_{com}\left(\frac{^{207}Pb_{com}}{^{206}Pb_{com}}\right)_{std}\left(\frac{^{206*}Pb}{^{238}U}\right)_{std}}{^{235}U_m}\right) = \left(\frac{^{206}Pb_m\left(\frac{^{207*}Pb}{^{235}U}\right)_{std}}{^{238}U_m}\right) - \left(\frac{^{206}Pb_{com}\left(\frac{^{207*}Pb}{^{235}U}\right)_{std}}{^{238}U_m}\right)$$

$$\left(\frac{^{206}Pb_{com}\left(\frac{^{207*}Pb}{^{235}U}\right)_{std}}{^{238}U_m}\right) - \left(\frac{^{206}Pb_{com}\left(\frac{^{207}Pb_{com}}{^{206}Pb_{com}}\right)_{std}\left(\frac{^{206*}Pb}{^{238}U}\right)_{std}}{^{235}U_m}\right) = \left(\frac{^{206}Pb_m\left(\frac{^{207*}Pb}{^{235}U}\right)_{std}}{^{238}U_m}\right) - \left(\frac{^{207}Pb_m\left(\frac{^{206*}Pb}{^{238}U}\right)_{std}}{^{235}U_m}\right)$$

Solve for $^{206}Pb_{com}$:

$$^{206}Pb_{com} = \frac{\frac{\left(^{206}Pb_m\left(\frac{^{207*}Pb}{^{235}U}\right)_{std}\right)}{^{238}U_m} - \frac{\left(^{207}Pb_m\left(\frac{^{206*}Pb}{^{238}U}\right)_{std}\right)}{^{235}U_m}}{\frac{\left(\frac{^{207*}Pb}{^{235}U}\right)_{std}}{^{238}U_m} - \frac{\left(\left(\frac{^{207}Pb_{com}}{^{206}Pb_{com}}\right)_{std}\left(\frac{^{206*}Pb}{^{238}U}\right)_{std}\right)}{^{235}U_m}} \qquad \text{(A2b)}$$

$^{206}Pb_{com}$ from **Equation A2a** or **A2b** can be substituted into **Equation A1a** to determine the fractionation factor for $^{207}Pb_m/^{235}U_m$. Note that $^{206}Pb_{com}$ occurs on both sides of **Equation A2a** or **A2b**. Three approaches may be employed to determine a value for $^{206}Pb_{com}$:

a) Directly measure $(^{207}Pb_{com}/^{206}Pb_{com})_{std}$ for the sample of interest. This can be done using a primary, co-genetic, U-poor phase such as potassium feldspar.
b) Measure $^{207}Pb_m$ and $^{206}Pb_m$ for multiple spots from a co-genetic suite of crystals. If sufficient variation in the relative amounts of $^{207}Pb_{com}$ and $^{206}Pb_{com}$ exists between the spots, the $(^{207}Pb_{com}/^{206}Pb_{com})_{std}$ can be determined from the y-intercept of a Tera-Wasserburg concordia plot of the *Pb* and *U* isotopic data.
c) A value of $(^{207}Pb_{com}/^{206}Pb_{com})_{std}$ can be assumed or calculated. One approach is to calculate the unique combination of t_{std} and $(^{207}Pb_{com}/^{206}Pb_{com})_{std}$ using a common Pb model such as Stacey and Kramers (1975). A similar approach can be used to calculate the age and common Pb values for apatite grains other than age standards.

Function `f207` below evaluates **Equation A1a** and function `f206` evaluates **Equation A1b (**Microsoft Corporation Visual Basic source code):

```
Function f207(Pb206, Pb207, U235, U238)
     Dim a1, a2 as single
     'Pb206=measured Pb206 value for standard
     'Pb207=measured Pb207 value for standard
     'U235=measured or calculated U235 value for standard
     'U238=measured U238 value for standard
     'Std206238Ratio=natural Pb206/U238 ratio for standard
     'Std207235Ratio=natural Pb207/U235 ratio for standard
     'Std207206Ratio=natural Pb207/Pb206 ratio for standard
     a1 = Std207235Ratio * Pb206 / U238
     a1 = a1 - Std206238Ratio * Pb207 / U235
     a2 = Std207235Ratio / U238
     a2 = a2 - Std206238Ratio * Std207206Ratio / U235
     f207 = Std206238Ratio / ((Pb206 - (a1 / a2)) / U238)
End Function

Function f206(R, Pb206, Pb207, U235, U238)
```

```
     'R=registration efficiency ratio Pb207/Pb206
     f206 = R * f207(Pb206, Pb207, U235, U238)
End Function
```

Fractionation Factor Normalization

```
Sub fnormalize(f206, f207, fPb)
     'normalize f206 f207 fPb
     'Std206238Ratio=natural Pb206/U238 ratio for standard
     'Std207235Ratio=natural Pb207/U235 ratio for standard
     'Std207206Ratio=natural Pb207/Pb206 ratio for standard
     '137.88=natural U238/U235 ratio
     'back to 'measured' ratios
     f207 = Std207235Ratio / f207
     f206 = Std206238Ratio / f206
     fPb = Std207206Ratio / fPb
     'normalize
     f206 = (f207 * ((1 / 137.88)/ fPb) + f206) / 2
     f207 = f206 * fPb / (1 / 137.88)
     'back to FF
     f207 = Std207235Ratio / f207
     f206 = Std206238Ratio / f206
     fPb = Std207206Ratio / fPb
End Sub
```

Table C1. Isotopes analyzed for AFTUPb sessions (^{235}Uc was calculated from ^{238}U).

Isotope	Acquisition Time (s)	Detection Mode	Background Window Width for Smoothing (spots)[1]	Isotope	Acquisition Time (s)	Detection Mode	Background Window Width for Smoothing (spots)[1]
^{23}Na	0.001000	auto	max	^{141}Pr	0.001000	auto	max
^{24}Mg	0.001000	auto	max	^{146}Nd	0.001000	auto	max
^{27}Al	0.001000	auto	max	^{147}Sm	0.001000	auto	max
^{29}Si	0.001000	auto	min	^{151}Eu	0.001000	auto	max
^{31}P	0.001000	auto	min	^{157}Gd	0.001000	auto	max
^{32}S	0.001000	auto	min	^{159}Tb	0.001000	auto	max
^{35}Cl	0.003000	auto	min	^{163}Dy	0.001000	auto	max
^{39}K	0.001000	auto	min	^{165}Ho	0.001000	auto	max
^{43}Ca	0.003000	auto	max	^{166}Er	0.001000	auto	max
^{47}Ti	0.001000	auto	max	^{169}Tm	0.001000	auto	max
^{55}Mn	0.001000	auto	min	^{172}Yb	0.001000	auto	max
^{56}Fe	0.001000	auto	min	^{175}Lu	0.001000	auto	max
^{75}As	0.001000	auto	max	^{178}Hf	0.001000	auto	max
^{79}Br	0.003000	auto	min	^{202}Hg	0.012600	auto	min
^{88}Sr	0.001000	auto	max	^{204}Pb	0.150000	auto	min
^{89}Y	0.001000	auto	max	^{206}Pb	0.150000	auto	max
^{91}Zr	0.001000	auto	max	^{207}Pb	0.150000	auto	max
^{127}I	0.003000	auto	min	^{208}Pb	0.150000	auto	max
^{138}Ba	0.001000	auto	max	^{232}Th	0.012500	auto	max
^{139}La	0.001000	auto	max	^{238}U	0.012500	auto	max
^{140}Ce	0.001000	auto	max	^{235}Uc	0.012500	auto	max

Notes: [1]min=window 9 spots wide; max=window 49 spots wide

Table C2. Laser ablation system and mass spectrometer acquisition parameters.

Laser Ablation System	
Instrument	Resonetics RESOlution M-50
Laser Type	ArF Eximer 193 nm
Institution	Donelick Properties dba
Location	Viola Idaho U.S.A.
Ablation Duration	34000 ms
Delay 1	6000 ms TTL
Delay 2	TTL 20000 ms
Laser Repetition Rate	5.0 Hz (AFTUPb_11_12_08-10) 7.0 Hz (AFTUPb_11_12_18-19)
Ablation Type	26 micron diameter spot
Attenuation	0.5
Stabilization Mode	constant energy 12.6 kV
Carrier Gas 1	650 mL/min ultra high purity He
Carrier Gas 2	2.0 mL/min ultra high purity N2
Stage Position Correction	Donelick Properties dba proprietary correction
Operator	Margaret B. Donelick
Technical Assistance	Raymond A. Donelick
Mass Spectrometer	
Instrument	Agilent 7700x
Mass Spectrometer Type	quadrapole ICP-MS
Institution	Donelick Properties dba
Location	Viola Idaho U.S.A.
Carrier Gas	5.20 kPa 1.0 L/min high purity Ar
Reflected Power	31 W
Forward Power	1320 W
Operator	Margaret B. Donelick
Technical Assistance	Raymond A. Donelick

Table C3. Apatite age standards.

Standard	Standard/Type	U-Pb age (±2σ)	[U] [Th] [Sm]	References
91500	91500	1065.4 ± 0.6 Ma		U-Pb age: Wiedenbeck et al. (1995); Yuan, H.-L. et al. (2008)
DR	Durango/ FT zeta and U-Pb secondary	31.44 ± 0.18 Ma	[U] = 12.1 ppm [Th] = 284 ppm [Sm] = 189 ppm	U-Pb age: McDowell et al. (2005) [U] [Th] [Sm]: Boyce and Hodges (2005) weighted means
FC	Duluth complex/ U-Pb tertiary	1099.0 ± 0.6 Ma		U-Pb age: Paces and Miller (1993)
F5	Duluth complex/ U-Pb secondary	1099.0 ± 0.6 Ma (assumed equal to FC-1)		U-Pb age: Paces and Miller (1993)
IF	Fish Canyon Tuff/ U-Pb tertiary	28.201 ± 0.012 Ma		U-Pb age: Lanphere et al. (2001); Kuiper et al. (2008)
MD	Mount Dromedary/ U-Pb tertiary	99.12 ± 0.14 Ma		U-Pb age: Renne et al. (1998)
MM	McClure Mountain/ U-Pb primary	523.98 ± 0.12 Ma	[U] = 23.2 ppm [Th] = 71 ppm [Sm] = 136 ppm	U-Pb age: Shoene and Bowring (2006) [U] [Th] [Sm]: based on Boyce and Hodges (2005) for DR Ap AFTUPb020711 and AFTUPb021411
MT	Mud Tank carbonatite	732 ± 5 Ma		U-Pb age: Black and Gulson (1978); Yuan, H.-L. et al. (2008)
OL	Otter Lake/ U-Pb tertiary	913 ± 7 Ma		U-Pb age: Barfod et al. (2005)
TI	Tioga Bed B/ U-Pb tertiary	390.5 ± 0.5 Ma		U-Pb age: Roden et al. (1990)

Table C4. Apatite fission track and U-Pb data (as Excel file with 3 tabs for each sample: filename is "Appendix C, Table C4, apatite FT and U-Pb data").

Figure C1a. Isotope ^{43}Ca, spot1711D_1, session AFTUPb_11_12_08-10: red: B_{scan} values (scans 1-13) and SB_{scan} values (scans 18-53); blue: S_{scan} values (scans 18-53).

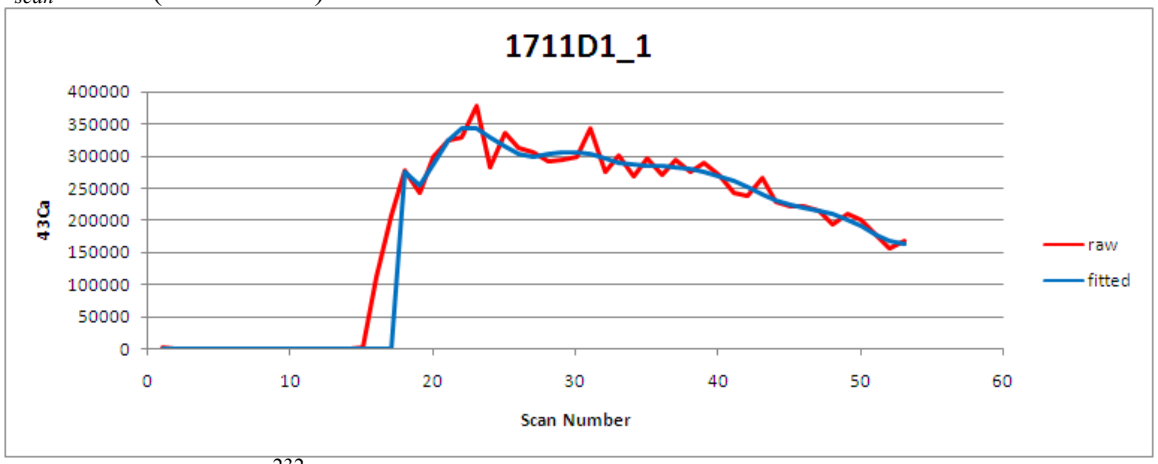

Figure C1b. Isotope ^{232}Th, spot1711D_1, session AFTUPb_11_12_08-10: red: B_{scan} values (scans 1-13) and SB_{scan} values (scans 18-53); blue: S_{scan} values (scans 18-53).

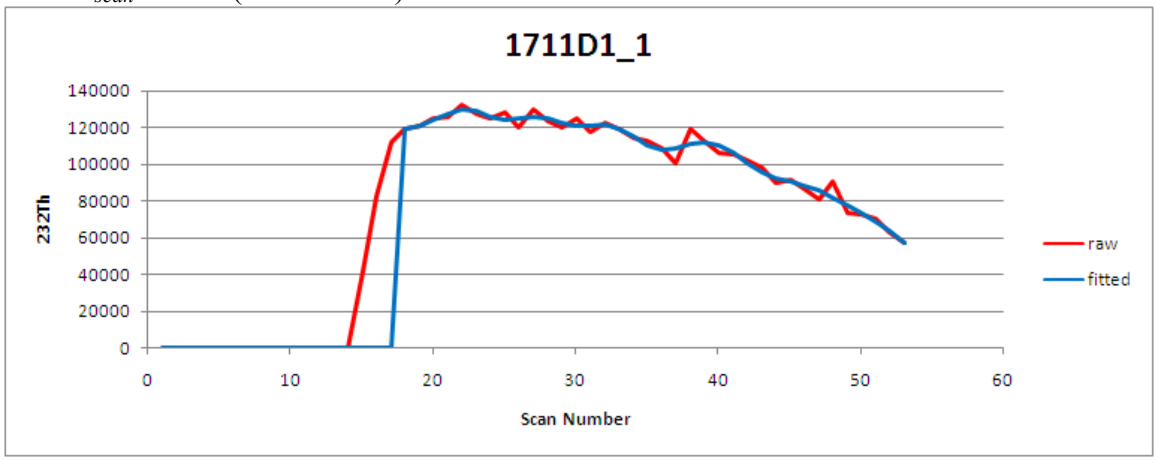

Figure C2a. Isotope ^{35}Cl, session AFTUPb_11_12_08-10: blue B_{spot} values; red: B_{spot_smooth} values (deflections to zero indicate failed analyses).

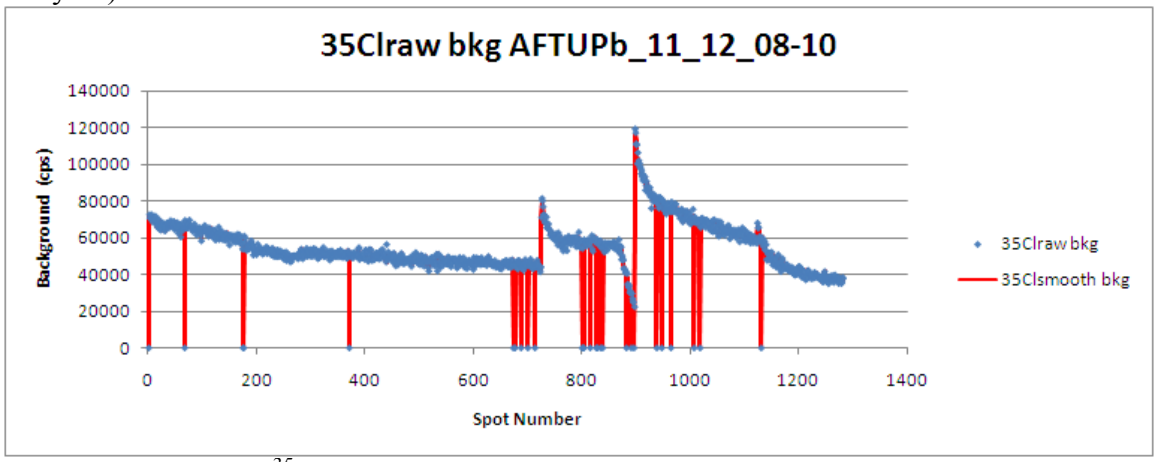

Figure C2b. Isotope ^{35}Cl, session AFTUPb_11_12_18-19: blue B_{spot} values; red: B_{spot_smooth} values (deflections to zero indicate failed analyses).

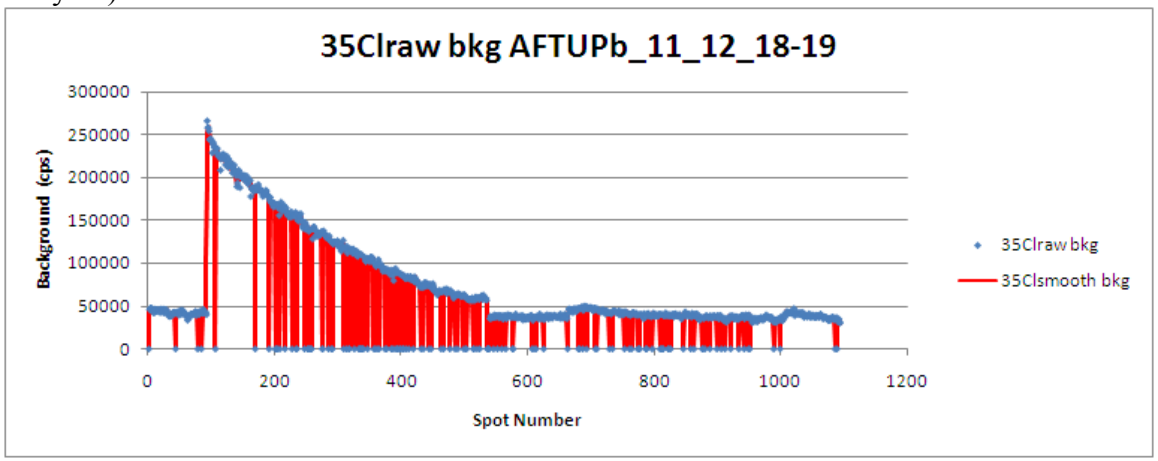

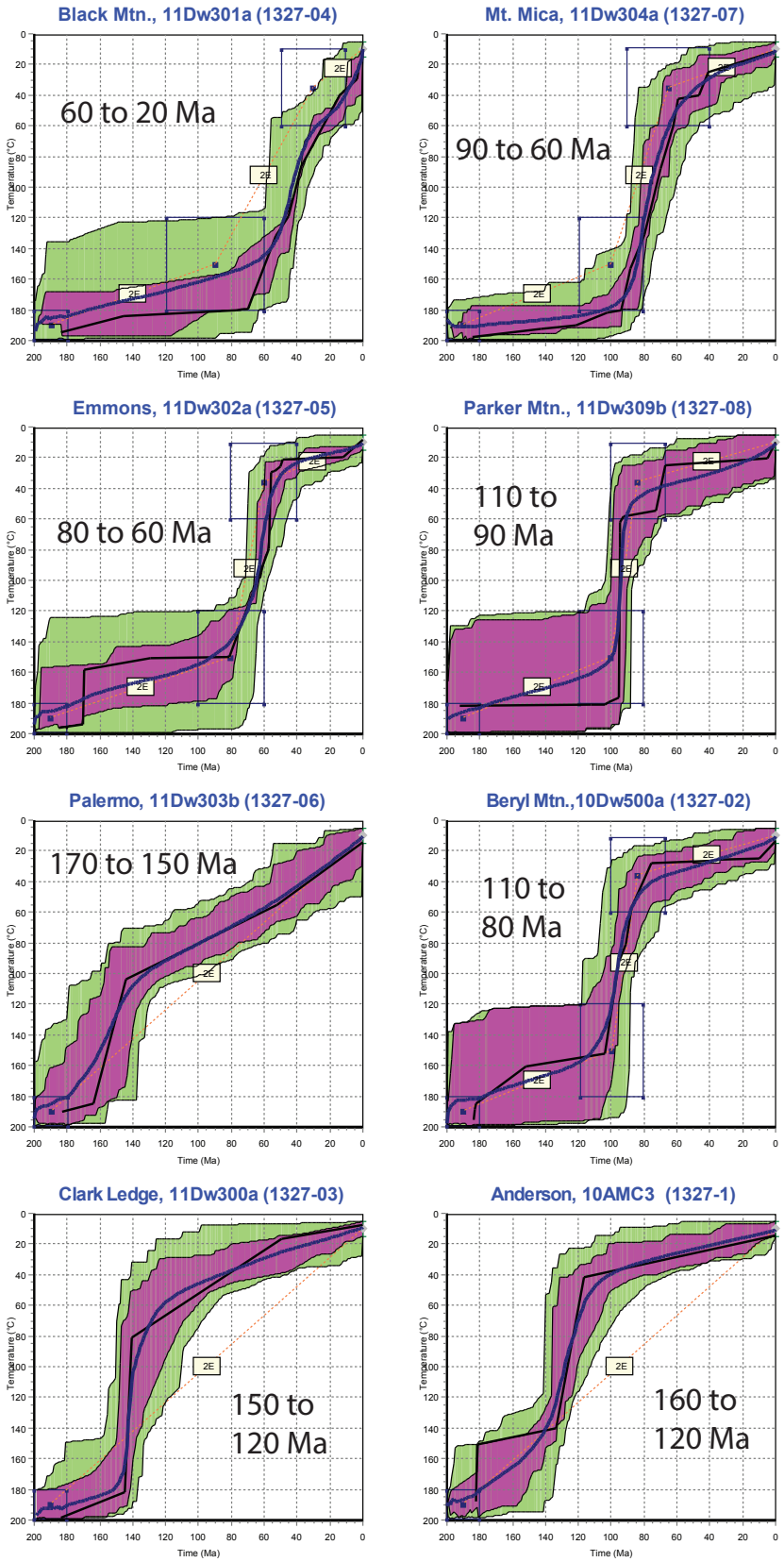

Fig. C3, Bradley et al., New England pegmatite geochronology—Appendix C

REFERENCES CITED IN THE APPENDICES A, B, AND C

Barfod, G.H., Krogstad, E.J., Frei, R. & Albarede, F. (2005) Lu-Hf and PbSL geochronology of apatites from Proterozoic terranes: A first look at Lu-Hf isotopic closure in metamorphic apatite. *Geochimica et Cosmochimica Acta* **69**, 1847-1859.

Black, L.P. Gulson, B.L. (1978) The age of the Mud Tank carbonatite, Strangways Range, Northern Territory. *BMR Journal Australian Geology and Geophysics* **3**, 227-232.

Black, L.P., Kamo, S.L., Allen, C.M., Davis, D.W., Aleinikoff, J.N., Valley, J.W., Mundil, R., Campbell, I.H., Korsch, R.J., Williams, I.S. & Foudoulis, C. (2004) Improved $^{206}Pb/^{238}U$ microprobe geochronology by the monitoring of trace-element related matrix effect; SHRIMP, ID-TIMS, ELA-ICP-MS and oxygen isotope documentation for a series of zircon standards. *Chemical Geology* **205**, 15-140.

Bowring, J.F., McLean, N.M. & Bowring, S.A. (2011) Engineering Cyber Infrastructure for U-Pb Geochronology: Tripoli and U-PbRedux: *Geochemistry, Geophysics, Geosystems* **12**, Q0AA19,DOI:10.1029/2010GC003479.

Boyce, J.W. & Hodges, K.V. (2005) U and Th zoning in Cerro de Mercado (Durango, Mexico) fluorapatite: Insights regarding the impact of recoil redistribution of radiogenic ^{4}He on (U-Th)/He thermochronology. *Chemical Geology* **219**, 261-274.

Carlson, W.D., Donelick, R.A. & Ketcham, R.A. (1999) Variability of apatite fission-track length annealing kinetics I: Experimental results. *American Mineralogist* **84**, 1213-1223.

Chang, Z., Vervoort, J.D., McClelland, W.C. & Knaack, C. (2006) U-Pb dating of zircon by LA-ICP-MS. *Geochemistry, Geophysics, Geosystems* **7**, 14 pp.

Chew, D.M., Sylvester, P.J. & Tubrett, M.N. (2011) U-Pb and Th-Pb dating of apatite by LA-ICPMS. *Chemical Geology* **280**, 200-216.

Deer, W.A., Howie, R.A. & Zussman, J. (1966) An Introduction to the Rock-Forming Minerals. John Wiley and Sons, Inc., New York, 528 p.

Donelick, R.A., O'Sullivan, P.B. & Ketcham, R.A. (2005) Apatite fission track analysis: *Reviews in Mineralogy and Geochemistry* **58**, 49-93.

Gehrels, G.E., Valencia, V.A. & Ruiz, J. (2008) Enhanced precision, accuracy, efficiency, and spatial resolution of U-Pb ages by laser ablation-multicollector-inductively coupled plasma-mass spectrometry. *Geochemistry Geophysics Geosystems* **9**, 1-13.

Gerstenberger, H. & Haase, G. (1997) A highly effective emitter substance for mass spectrometric Pb isotope ratio determinations. *Chemical Geology* **136**, 309-312.

Hasebe, N., Barbarand, J., Jarvis, K., Carter, A. & Hurford, A.J. (2004) Apatite fission-track chronometry using laser ablation ICP-MS. *Chemical Geology* **207**, 135-145.

Hunt, C.B. (1958) Structural and igneous geology of the La Sal Mountains, Utah. *U.S. Geoloogical Survey Professional Paper* **294-I**, 305-364.

Hurford, A.J. & Green, P.F. (1983) The zeta age calibration of fission-track dating. *Isotope Geoscience* **1**, 285-317.

Hurford, A.J. & Green, P.F. (1982) A users' guide to fission track dating calibration. *Earth and Planetary Science Letters* **59**, 343-354.

Ketcham, R.A. (2005) Forward and inverse modeling of low-temperature thermochronometry data. *Reviews in Mineralogy and Geochemistry* **58**, 275-314.

Ketcham, R.A., Donelick, R.A. & Carlson, W.D. (1999) Variability of apatite fission-track annealing kinetics, III, Extrapolation to geological time scales. *American Mineralogist* **84**, 1235-1255.

Ketcham, R.A., Donelick, R.A. & Donelick, M.B. (2000) AFTSolve: a program for multi-kinetic modeling of apatite fission-track data. *Geological Materials Research* **2**(1), 1.

Krogh, T.E (1973) A low-contamination method for hydrothermal decomposition of zircon and extraction of U and Pb for isotopic age determinations. *Geochimica et Cosmochimica Acta* **37**, 485-494.

Kuiper, K.F., Deino, A., Hilgen, P.J., Krijgsman, W., Renne, P.R., and Wijbrans, J.R., 2008. Synchronizing rock clocks of Earth history. Science, 320, p. 500-504.

Lanphere, M.A. & Baadsraard, H. (2001) Precise K-Ar, $^{40}Ar/^{39}Ar$, Rb-Sr and U-Pb mineral ages from the 27.5 Ma Fish Canyon Tuff reference standard. *Chemical Geology* **175**, 653-671.

Lanphere, M.A. & Dalrymple, G.B. (2000) First-principles calibration of ^{38}Ar tracers: Implications for the ages of $^{40}Ar/^{39}Ar$ fluence monitors. U.*S. Geological Survey Professional Paper* **1621**, 1-10.

Layer, P.W. (2000) Argon-40/argon-39 age of the El'gygytgyn impact event, Chukotka, Russia. *Meteoritics and Planetary Science* **35**, 591-599.

Layer, P.W., Hall, C.M. & York, D. (1987) The derivation of $^{40}Ar/^{39}Ar$ age spectra of single grains of hornblende and biotite by laser step heating. *Geophysical Research Letters* **14**, 757-760.

Ludwig, K.R. (2003) Isoplot 3.00, A Geochronological Toolkit for Microsoft Excel: University of California at Berkeley, kludwig@bgc.org.

Mattinson, J.M. (2005) Zircon U–Pb chemical abrasion (''CA–TIMS'') method: combined annealing and multi-step dissolution analysis for improved precision and accuracy of zircon ages. *Chemical Geology* **220**, 47–66. doi:10.1016/j.chemgeo.2005.03.011.

Mattinson, J. M., 2010, Analysis of the relative decay constants of ^{235}U and ^{238}U by multi-step CA-TIMS measurements of closed-system natural zircon samples: Chemical Geology, v. 275, p. 186-198.

Mattinson, J.M. (2011) Extending the Krogh legacy: development of the CA–TIMS method for zircon geochronology. *Canadian Journal of Earth Sciences* **48**, 95–105.

McDougall, I. & Harrison, T.M. (1999) Geochronology and Thermochronology by the $^{40}Ar/^{39}Ar$ method-2nd ed, Oxford University Press, New York, 269 pp.

McDowell, F.W., McIntosh, W.C. & Farley, K.A. (2005) A precise $^{40}Ar/^{39}Ar$ reference age for the Durango apatite (U-Th)/He and fission-track dating standard. *Chemical Geology* **214**, 249-263.

McLean, N.M., Bowring, J.F. & Bowring, S.A. (2011) An Algorithm for U-Pb Isotope Dilution Data Reduction and Uncertainty Propagation. *Geochemistry, Geophysics, Geosystems* **12**, Q0AA18, DOI:10.1029/2010GC003478.

Paces, J.B. & Miller, J.D. (1993) Precise UPb ages of Duluth Complex and related mafic intrusions, northeastern Minnesota: Geochronological insights to physical, petrogenic, paleomagnetic, and tectonomagmatic processes associated with the 1.1 Ga Midcontinent Rift System. *Journal of Geophysical Research* **98**, 13997-14013.

Paton, C., Woodhead, J.D., Hellstrom, J.C., Hergt, J.M., Greig, A. & Maas, R. (2010) Improved laser ablation U-Pb zircon geochronology through robust downhole fractionation correction.: *Geochemistry, Geophysics, Geosystems* **11**, Q0AA06, doi:10.1029/2009GC002618.

Renne, P.R., Swisher, C.C., Deino, A.L., Karner, D.B., Owens, T.L. & DePaolo, D.J. (1998) Intercalibration of standards, absolute ages and uncertainties in $^{40}Ar/^{39}Ar$ dating. *Chemical Geology* **45**, 117-152.

Roden, M.K., Parrish, R.R. & Miller, D.S. (1990) The absolute age of the Eifelian Tioga ash bed. *The Journal of Geology* **98**, 282-285.

Roeder, P.L., MacArthur, D., Ma, X.-P., Palmer, G.R. & Mariano, A.N. (1987) Cathodoluminescence and microprobe study of rare-earth elements in apatite. *American Mineralogist* **72**, 801-811.

Rogers, P.S.Z., Duffy, C.J., Benjamin, T.M. & Maggiore, C.J. (1984) Geochemical applications of nuclear microprobes. *Nuclear Instruments and Methods in Physics Research* **B3**, 671-676.

Rønsbo, J.G. (1989) Coupled substitutions involving REEs and Na and Si in apatites in alkaline rocks from the Ilimaussaq intrusion, South Greenland, and the petrological implications. *American Mineralogist* **74**, 896-901.

Samson S.D. & Alexander E.C. (1987) Calibration of the interlaboratory $^{40}Ar/^{39}Ar$ dating standard, MMhb1. *Chemical Geology* **66**, 27-34.

Schoene, B. & Bowring, S.A. (2006) U-Pb systematics of the McClure Mountain syenite: thermochronological constraints on the age of the $^{40}Ar/^{39}Ar$ standard MMhb. *Contributions to Mineralogy and Petrology* **151**, 615-630.

Stacey J.S. & Kramer J.D. (1975) Approximation of terrestrial lead isotope evolution by a two-stage model. *Earth and Planetary Science Letters* **26**, 207-221.

Steiger, R.H. & Jaeger, E. (1977) Subcommission on geochronology: Convention on the use of decay constants in geo and cosmochronology, *Earth and Planet Science Letters* **36**, 359-362.

Weidenbeck, M., Alle, P., Corfu, F., Griffin, W.L., Meier, M., Oberli, F., Vonquandt, A., Roddick, J.C. & Speigel, W. (1995) Three natural zircon standards for U-Th-Pb, Lu-Hf, trace-element and REE analyses. *Geostandards Newsletter* **19**, 1-23.

York, D., Hall, C.M., Yanase, Y., Hanes, J.A. & Kenyon, W.J. (1981) $^{40}Ar/^{39}Ar$ dating of terrestrial minerals with a continuous laser. *Geophysical Research Letters* **8**, 1136-1138.

Young, E.J., Meyers, A.T., Munson, E.L. & Conklin, N.M. (1969) Mineralogy and geochemistry of fluorapatite from Cerro de Mercado, Durango, Mexico. *U.S. Geological Survey Professional Paper* **650-D**, D84-D93.

Yuan, H.-L., Gao, S., Dai, M.-N., Zong, C.-L., Günther, D., Fontaine, G.H., Liu, X.-M. & Diwu, C. (2008) Simultaneous determinations of UPb age, Hf isotopes and trace element compositions of zircon by excimer laser-ablation quadrapole and multiple-collector ICP-MS. *Chemical Geology* **247**, 100-118.

Zhang, M., Ewing, R.C., Boatner, L.A., Salje, E.K.H., Weber, W.J., Daniel, P., Zhang, Y. & Farnan, I. (2009) Pb* irradiation of synthetic zircon ($ZrSiO_4$): Infrared spectroscopic study – Reply. *American Mineralogist* **94**, 856-858.